Point-by-point reply to review comments on ‘Dynamic changes on Wilkins Ice Shelf during the 2006-2009 retreat derived from satellite observations’ by Rankl et al.

The authors want to thank both reviewers for their careful reading of the manuscript. The comments were very useful and helped to improve the manuscript substantially. Large parts of the manuscript have been re-structured following the suggestions given by Ted Scambos. More methodological aspects brought up by Reinhard Drews have been addressed extensively in the revised version of the manuscript. In the following, all comments are addressed specifically and changes in the manuscript indicated. We hope, both reviewers support the changes made in the revised manuscript.

Comments by Reinhard Drews

Summary
Ice shelves buttress ice flowing off the Antarctic continent, and ice-shelf disintegration causes a rapid increase in ice discharge. To predict the future of ice shelves, it is important to derive metrics assessing ice-shelf stability from observations. The Wilkins Ice Shelf (Antarctic Peninsula) has shown significant dynamic changes over the last decades, including thinning and frontal retreat, making it a suitable test case for previously published metrics such as the ’compressive arch’ (Doake et al. 1998) or the ’stress-flow angles’ (Kulessa et al., 2014).

With this motivation in mind, Rankl et al. present 8 time-slices of surface velocities for the Wilkins Ice Shelf starting in 1994 and ending in 2010. The velocities were derived using intensity/speckle tracking on scenes from various radar satellite sensors. Based on the surface velocities, they derive strain rate fields and the corresponding magnitude/direction of the principal strain rates. Using a simplified rheology (which assumes a spatially/temporally constant rate factor), they also derive the corresponding stress fields with the direction/magnitude of the principal stresses. The surface velocities quantify temporal changes, in particular an acceleration in 2008 as response to a partial disintegration of an ice bridge between Latady and Charcot Island. Crevasse formation and frontal retreat are tracked in the underlying backscatter images. The derived strain rate and stress fields provide temporally resolved data for testing ice-shelf stability criteria. The authors find that the first principle strain rate (direction of maximum extension) describes observed crevasse opening and the corresponding principal stresses give some indication at which threshold this may occur (subject to the simplified rheology). Change of sign in the second principal stress are independent of the rate factor and help during the interpretation. In particular, positive second principal stresses (marking a purely extensive flow regime) seem to mark areas which are prone to disintegrate. Other measures such as the second strain-rate invariant of the stress-flow angles remain ambiguous.

General Impression
The time series of surface velocities provide a strong observational dataset quantifying the dynamic changes of the Wilkins Ice Shelf in the past. I appreciate the derivation of strain rates and stresses (together with their principal components) to understand the underlying mechanisms of ice-shelf stability which is a timely and important topic. Overall I enjoyed reading this manuscript and from my point of view, this paper will fulfill the standards of The Cryosphere. Below I do suggest some revisions which should be addressed and which hopefully will help to improve the final version of the paper. I hope the authors persever to go through my comments, and to turn this already well-developed TCD paper into a nice TC publication.
Reinhard Drews

General Comments

1. The paper is in many places unnecessarily descriptive where it could be rigorous. This is manifested in expressions such as "some of the measures [..] emerge to be more or less applicable" p.7/l.29 (is it applicable or not, and why?), "..acceleration is somewhat lower" (how much?), "..showed very small velocities in March.." (how slow and slow compared to what?). Although the individual examples are all minor, the repeated

occurrence of these type of descriptions makes the paper imprecise and speculative in places. Below I mention a detailed list and suggest improvements.

Ted Scambos asked for a profound re-organization of the Results section. During the rewriting, we tried to remove many of these imprecise and ambiguous formulations.

2. Error estimates of the velocities are derived in the supplements, but I wonder if these errors are complete. From my experience with intensity tracking, it is (at least sometimes) required to calibrate the data (e.g. offset it at rock outcrops) and even the calibrated fields may show non-zero, spatially varying values in the difference fields of mosaics (due to errors in coregistration, orbital information, atmospheric contribution,...).

We thank the reviewer for this comment. The reviewer is right that additional calibration of the velocity fields might be useful in some cases. We did not do any additional subtraction of measured offsets on stable ground as the reviewer suggests. However, we think that the full possible error contribution is expressed in the term σ_v^C. This value captures all errors related to the co-registration procedure and is hence, larger than an error that would have been assessed after additional calibration. Further error contribution related to the orbital information or the atmospheric influence is hard to estimate, however, we would welcome any suggestions to do so. We think the error estimation over non-moving areas as a reference is a standard procedure when using intensity-offset tracking methods (Burgess et al., 2012; McNabb et al., 2012; Quincey et al., 2009, 2011; Seehaus et al., 2015). The second value σ_v^T, which adds to the error calculation considers further error sources related to the tracking algorithm, the spatial resolution and time interval of image acquisitions and, in our opinion, improves the overall error estimation. In a revised manuscript, we will address the error computations in more detail as suggested by the reviewer.

In Fig. 2b,c,d,e cutting edges are visible, but the authors do not report their magnitude and attribute them to monthly flow variations. With the information available in the paper, this appears overinterpreted and should be better justified (how were the data calibrated, what is the magnitude of the cutting edges and what other evidence exists for monthly flow variations?). Along those lines, I suggest to show the full difference field and not restrict it to the western part only.

During the preparation of the velocity results, we first tried to calibrate the single velocity fields to each other. However, due to the mostly structureless ice shelf with in some parts very few non-moving areas, only limited overlapping areas could be identified to be used for calibration. The offsets between tracks are also not linear (range between 3 and 18 m/yr) and hence, a subtraction is not a straight forward approach without sufficient reference on stable ground. Our efforts did not lead to substantially more consistent velocity fields when also considering the offsets on stable ground. Since there are no in-situ measurements on WIS and only limited satellite data coverage suitable for intensity-offset tracking or interferometry, we cannot give more details on short-term velocity variations. In addition, this is also the reason for varying co-registration accuracies during offset racking. Hence, we decided against further calibration and to show the ‘as is’ flow fields, which might show short-term flow variations or, as the reviewer correctly pointed out, processing artefacts. In a revised version of the paper, we will address this point more clearly and explain the reasons for our approach and give values of the offsets. We also decided against any coarse smoothing techniques as often applied to large scale ice sheet velocities, in order to keep as much detail as possible. The cutting edges are also the reason, why we have decided to show flow differences for the western part of the ice shelf only. This part of the ice shelf is most important for the aim of our paper, since dynamic changes due to frontal break-up are obvious in this part, whereas the eastern part of the ice shelf is not influenced mainly due to the blocking effect of numerous ice rises.

3. The wave-like pattern which appears in the strain rates (e.g. Fig. 2 c,k,o) and elsewhere is quite prominent but is only briefly mentioned in an isolated sentence (p. 6/l. 12) when describing the stresses. This must be mentioned earlier (e.g. section 3.1) and the explanation should be expanded. How is it possible that the tracking algorithm creates such a pattern, and if so, why only in the scenes from 2008 and 2009? Ionospheric path delays are possible but may not be the only option. Somewhat immodestly I refer to Drews et al. 2009 (IEEE Geosc. Rem. Sens. Fig. 4) where a similar wave-like pattern has been linked to variations in troposhperic water vapor content. However, this was using differential SAR interferometry and I don’t know how this would appear in flow fields based on intensity/speckle tracking.

We thank the reviewer for this advice and will discuss this in more detail in an updated manuscript. We also agree that the tracking algorithm is the most unlikely source for these patterns due to the reasons mentioned by the reviewer. Other publications have found comparable patterns in ice velocities derived from intensity tracking and related them to fluctuations in the polar ionospheric electron density (e.g., Gray et al., 2000; Joughin, 2002; Nagler et al., 2015). These fluctuations affect not only the interferometric phase, but also a mismapping of the azimuth pixel position (Gray et al., 2000). Especially slow moving areas are affected by these patterns, which is true for the WIS. The proposed wavelength of the pattern of 5-10 km is applicable to WIS (Gray et al., 2000). An improvement by averaging the flow fields over multiple acquisitions as proposed in Nagler et al. (2015) is not possible in our case due to lack of further, suitable image pairs. Solar activity is strongly variable in time and would hence explain why we observe the pattern only on a few image pairs.
We are thankful about the advice mentioning the possible influence of the tropospheric water vapor content. This is certainly another temporarily variable source of error. However, related studies have mentioned an influence on C-Band InSAR only (Williams et al., 1998), which is a more sensitive technique on the path delays due to water vapor. We will include this as another possible reason for the observed pattern, although we did not find further information about any effects on the results derived from intensity tracking. In our view, ionospheric disturbances remain the most likely reason for the observed patterns.

4. I have no prior experience in applying the ice-shelf stability criteria mentioned in the manuscript and I enjoyed learning more about them. However, in the end I was left with a foggy impression which criteria are applicable where and under which conditions. A good example for this confusion is the paragraph p.7/l. 38f stating that the authors "want to follow Doak et al. (1998)" in saying that "when the ice front retreats beyond a certain isoline [in the second principal strain rates] destabilization is expected". However, two sentences later it is stated that the observed "second principal strain rates are [..] insensitive during the retreat of WIS" which makes me think that the Doak-criteria does not fit because WIS has retreated. However, the authors go on stating that the "negative values suggest general recession" which again is what has been observed. I am sure that I misunderstand something here, but even after reading this paragraph multiple times I am still left in the dark whether or not the second principal strain rates are a good or a bad metric for assessing the stability in this case. Similar ambiguities also occur at other places mentioned below. Summarizing, I am not questioning the analysis, but I suggest that the authors put more effort into clearly stating their findings which are currently partially hidden. This also includes sharpening the conclusions. Detailed comments are mentioned below.
The reviewer's comment again points out imprecise formulations, which we hopefully could improve by largely rewriting the Results section. The specific section now reads as follows:
'For the interpretation of the second principal strain-rate component (Fig. 3, lowest panels), we want to follow Doake et al. (1998). They forwarded that when the ice front retreats beyond a certain 'compressive arch', the ice-shelf integrity is no longer granted and destabilization is expected. This strain-rate arch separates a seaward area of extension from an inland area of compression. The stress value associated to the 'compressive arch' isoline is not well quantified but "is probably close to the transition from extension to compression" (Doake et al., 1998) and thus, close to the zero isoline of the second principal strain-rate. On WIS, values are generally negative indicating unstable conditions, which is confirmed by general retreat. Yet, the threshold isoline is not clearly specified and might change in time and differ between ice shelves. Moreover, the second principal strain-rate field is found to be not very sensitive to ice-shelf fracturing and gradual ice-front recession, which appears unfavourable when assessing the dynamic state of an ice shelf.'

Specific Comments
p1 l 12 how about "A total area of 2135±75km 2 (Xxpercent of the total ice shelf area)
The corresponding value has been added to the text.
p1 l 12 "multi-temporal": how about "in order to derive temporal variability of surface flow
The sentence has been changed into:
'The present study uses time-series of SAR satellite observations (1994/96, 2006-2010) in oder to derive variations in surface flow speed from intensity offset tracking methods.'
p1 l 14 "which were forwarded" – > "which were forwarded previously"
This sentence has been removed during rewriting.
p1 l 21 "pins down" –> "defines"

This sentence has been removed.

p1 l 22 remove "general"

This sentence has been removed.

p1 l 23 ice-shelf "disintegration" "collapse" "break-up" are used interchangeably. Maybe better stick to one term if you mean the same thing to avoid confusion for the reader. Same for ice-front "retreat" "recession"

We tried to clear the terminology in the text and hope it is less confusing now.

p1 l 26 I have difficulties imagining a tongues of a tributary glacier feeding into an ice shelf. Can you clarify?

We are not really sure what the reviewer is referring to.

p1 l 33 I supposed "within only one week" refers to the time period of ice-shelf disintegration. It could also mean that the criterion was published on week after the breakup. Rephrase.

This sentence has been changed accordingly.

p2 l 9: "under" –> "during"

This sentence has been changed accordingly.

p2 l 26: "multi-temporal" –> "time series"

This sentence has been changed accordingly.

p2 l 35: I suggest to mention also normalized values of the area (e.g. relative to the entire ice-shelf extent in year XX), because it is hard to get a feel for these numbers otherwise.

The corresponding value has been added to the text.

p2 l 38: Surface melt ponding may still play a role in ice-shelf disintegration. Stick a "exclusively" in there or restrict this sentence to the WIS. Otherwise you neglect the role of surface-melt ponding in general, which I think is not what you intend.

This sentence has been changed accordingly.

p3 l 19: Compared to which reference direction are flow vectors filtered? Where does this direction come from?

As proposed in Burgess et al. (2012) the offset fields were filtered for unreasonable values by using an efficient algorithm that compares the orientation and magnitude of a displacement vector in respect to its surrounding vectors. In terms of flow direction this means, that each flow vector in a predefined moving window (here: 5x5 pixels) is compared to the orientation assigned to the window's center pixel. For this, thresholds of 20, 18 and 12 degrees were chosen (Burgess et al., 2012). In an iterative process, each vector which deviates from the defined threshold was deleted.

p3 l 16: specify what you mean with "relative orbits" as opposed to just "orbits".

A relative orbit can be compared to e.g. the Landsat path number. It describes the repeating coverage of a satellite. For better understanding we changed the manuscript and used another term for this (applies also to next comment).

p3 l 21f: I get the feeling that "relative" refers to uncalibrated data where as "absolute" refers to calibrated data. Please specify how the calibration was done (on rock outcrops?) and be more clear about using the words relative/absolute

The authors apologize for the misleading phrasing. The text referred to the satellite's repeating flight path (relative), and the absolute magnitude of the derived flow fields (compared to relative magnitudes derived from e.g. InSAR). This section was changed for better understanding.

p3 l 5 : What is the final gridding of the velocities and did you apply any calibration?

The final gridding of the velocity fields is 50x50 m. This information has been added to the text. The co-registration procedure relies on the masked intensity images, i.e. non-moving areas such as bedrock and ice rises. Hence, we did not apply any further calibration of the velocity fields, since the co-registration accuracy was at a high level.

p3 l 25: I am not yet convinced that the deviations in the overlapping parts of the mosaicked surface flow are solely due to monthly ice-flow variations. Are there any independent data showing that ice-flow varies on monthly time scales and by how much? How can you be sure that the observed offsets are not due to the processing artefacts (i.e. unresolved coregistration offsets, imprecise orbital information or maybe even atmospheric contributions)? I think this point should be discussed in more detail, because the difference field is a major result of this paper. Currently I have the feeling that the overall data accuracy of the velocities is overestimated (although Fig. 2g is and will remain significant). I am happy to be shown otherwise.

See comment above.

p3 l 25: Given that TC has no rigid page limit, I don't see the advantage of having the error analysis (which I find important) in the supplements.

The description of the error estimation has been added to the manuscript.

p4 l 11: Pattyn 2003 is a paper about including higher-order mechanics in ice-flow models. However, the use of deviatoric stresses is more general and already occurs in the shallow ice approximation. Therefore, I find this reference a little misleading and suggest a textbook reference (Greve Blatter, Cuffey Patterson,…)

We changed the reference accordingly.

p4 l 12 "data are acquired" (data are plural)

The sentence has been changed accordingly.

p4 l 20 remove "In addition,"

The sentence has been changed accordingly.

p4 l 20 "necessarily linear" –> "is non-linear" (I consider this as the default in glaciology. The "not necessarily linear" somehow implies otherwise.)

The sentence has been corrected as suggested.

p4 l 25 Remove "generally". The rate factor always depends on temperature.

The sentence has been changed accordingly.

p4 l 30 Not sure if it is fully correct to state the "stress tensor" is symmetric by construction. The symmetry reflects conservation of angular momentum. I don't want to be witty here, just point out small imprecise language. Maybe rephrase.

The reviewer's comment points at a small detail which we certainly want to accommodate. The passage reads now as follows:

'Strain and stress components are real and respective tensors are symmetric which ultimately reflects the conservation of angular momentum in continuum mechanics.'

p4 l 34 E-5 (also at other places) is not TC style

The notation has been changed throughout the manuscript.

p5 l 5f: I am more used to have velocities in meters per year but certainly don't insist on it.

We would like to keep the velocity indications in meter per year and hope the reviewer is ok with this.

p5 l 11: Quantify "very small" because velocities are a main result of this paper there is no need to be descriptive here. Same holds for terms like "slightly higher" etc.

The sentence has been changed accordingly.

p5 l 13 "large double fracture" how large?

The fracture pair was about 45km long. This information was added to the text.

p5 l 17 "the consecutive acceleration was most expressed" how about "the consecutive acceleration was largest at.."

The sentence has been changed accordingly.

p5 l 18 "0.8 meters per day" is a velocity, not an acceleration. Do you mean velocity increase? Again, mentioning relative values (e.g. and XX percent increase) would help to better grasp the meaning of these numbers.

The sentence has been changed accordingly. The velocity increase nearly tripled at the narrowest part of the ice bridge. We hope the sentence is clearer now.

p5 l 19 terms like "somewhat lower" are unnecessarily descriptive for primary results. Same for "rather stagnant".

The first sentence mentioned here has been removed from the manuscript. Also, we deleted 'rather'.

p5 l 26: How about: "We calculate strain rates at each point in a local coordinate system with the two axis aligned parallel and perpendicular to the local flow direction."

Corrected following the reviewer's suggestion. We hope this clarifies how the in-flow strain rates are computed.

p5 l 26: Mention and check that the invariants (principal strain rates etc.) are indeed invariant compared to strain rates which are calculated in a global coordinate system.

The decomposition was already cross-checked by verifying that first principal components are larger than second principal components. For the strain-rates we additionally checked whether the values in flow direction fall between the minimum and maximum defined by the first and principal components.

p5 l 30: Which threshold was chosen and why? Fig. 3 mentions 0.05 m/d.

Yes, a threshold of 0.05 m/day was chosen here. This information has been added to the text here, we thank the reviewer for his careful reading. This threshold has been chosen based on the visual interpretation of the ice flow during image analysis. Flow directions in areas of magnitudes lower than 0.05 m/day weren't thoroughly convincing.

p5 l 33: "slight inflow"?

The corresponding sentence has been changed into:

'Additional inflow originating from Latady Island leads to compressive strain-rates further south.'

p6 l 2: a "certain direction" is imprecise. It is along the eigenvector corresponding to the eigenvalue.

This somewhat imprecise formulation was removed during re-structuring of the Results section.

p6 l 2: As a non-sailor I constantly mix up "lee" and "luv". Also people may understand this term from a perspective of atmospheric circulation. I think it is better to talk about "upstream" and "downstream" in these cases (and elsewhere).

We thank the reviewer for this advice. We changed the terminology for better understanding.

p6 l 6: quantify "less negative"

The sentence has been changed accordingly.

p6 l 14: This must be mentioned earlier and discussed in more detail (see general comment above).

An explanation has been added to the methods section.

p6 l 33 remove "more or less"

The sentence has been changed.

p6 l 35 when interpreting strain fields for fracture formation it is important to explicitly state the resolution of velocities and strain rates.

We thank the reviewer for this advice. The resolution of each resulting velocity field or derived quantity is 50x50m. We added this information to the respective methods part.

p7 l 16 "Even if zero is not passed, "–> "Even if values remain negative, …"

The sentence has been changed.

p7 l 29 "more or less" is not helpful here. Better write a clear sentence stating that no single stress/strain field can fully explain the observations (or something like that).

We changed the sentence for better understanding.

p7 l 30 I suggest avoiding "might be" (and "could be" later on) and instead clearly stating the uncertainties that are indicated with these formulations.

This paragraph has been re-formulated.

p7 l 36 I do not grasp the meaning of this paragraph and suggest rephrasing (see general comment above).

This paragraph has been re-structured.

p7 l 38 "certain" isoline? Is it not the 0 isoline specifying pure extension in all directions (as stated in intro)?

Doake et al. (1998) are very careful when formulating this criterion. Their figures somehow implicitly suggest that they mean the 0 isoline, but when describing the compressive arch, Doake et al. (1998) stay rather vague. There is no hard statement that the threshold is at zero. They only state that it might not deviate much from zero. Therefore we also kept their decision to not explicitly specify the zero isoline as the definition of the compressive arch. We changed the respective paragraph accordingly.

p7 l 38 "retreats/recedes" what is the difference between retreating and receding and why are both verbs mentioned here?

We opted for 'retreats' in this context.

p8 l 9 This paragraph of fractures fits to the one started in p7 l29. I also suggest to move the last paragraph of the conclusions to this section to have all fracture-related things together.

Intuitively, this comment was addressed during the re-organisation of the Results section. The passage in the conclusion was now added to the Results section where the gradual recession and evolution of WIS is recapitulated.

p 8 l 29: This paragraph brings up a observations which have not been discussed previously in the paper. I suggest not to introduce novel things in the conclusions (see previous comment).

See above answer.

p8 l 16 High variability or high uncertainty (because flow direction is ill-constrainedy?

These are uncertainties from the offset tracking that directly transmit into all derived fields. Errors are now explicitly indicated in the text.

Figure 1
I don't see the red nor the cyan line. On the other hand I see an orange ice-front position not mentioned in legend. Something went wrong here.
We are sorry for this mistake. The Figure has been changed and improved.

References

Burgess, E. W., Forster, R. R., Larsen, C. F. and Braun, M.: Surge dynamics on Bering Glacier, Alaska, in 2008–2011, The Cryosphere, 6(6), 1251–1262, doi:10.5194/tc-6-1251-2012, 2012.

Gray, A. L., Mattar, K. E. and Sofko, G.: Influence of ionospheric electron density fluctuations on satellite radar interferometry, Geophys. Res. Lett., 27(10), 1451–1454, doi:10.1029/2000GL000016, 2000.

Joughin, I.: Ice-sheet velocity mapping: a combined interferometric and speckle-tracking approach, Ann. Glaciol., 34(1), 195–201, 2002.

McNabb, R. W., Hock, R., O'Neel, S., Rasmussen, L. A., Ahn, Y., Braun, M., Conway, H., Herreid, S., Joughin, I., Pfeffer, W. T., Smith, B. E. and Truffer, M.: Using surface velocities to calculate ice thickness and bed topography: a case study at Columbia Glacier, Alaska, USA, J. Glaciol., 58(212), 1151–1164, doi:10.3189/2012JoG11J249, 2012.

Nagler, T., Rott, H., Hetzenecker, M., Wuite, J. and Potin, P.: The Sentinel-1 Mission: New Opportunities for Ice Sheet Observations, Remote Sens., 7(7), 9371–9389, doi:10.3390/rs70709371, 2015.

Quincey, D. J., Copland, L., Mayer, C., Bishop, M., Luckman, A. and Belo, M.: Ice velocity and climate variations for Baltoro Glacier, Pakistan, J. Glaciol., 55(194), 1061–1071, 2009.

Quincey, D. J., Braun, M., Glasser, N. F., Bishop, M. P., Hewitt, K. and Luckman, A.: Karakoram glacier surge dynamics, Geophys. Res. Lett., 38(18), L18504, doi:10.1029/2011GL049004, 2011.

Seehaus, T., Marinsek, S., Helm, V., Skvarca, P. and Braun, M.: Changes in ice dynamics, elevation and mass discharge of Dinsmoor–Bombardier–Edgeworth glacier system, Antarctic Peninsula, Earth Planet. Sci. Lett., 427, 125–135, 2015.

Williams, S., Bock, Y. and Fang, P.: Integrated satellite interferometry: Tropospheric noise, GPS estimates and implications for interferometric synthetic aperture radar products, J. Geophys. Res., 103(B11), 27051–27067, 1998.

Point-by-point reply to review comments on 'Dynamic changes on Wilkins Ice Shelf during the 2006-2009 retreat derived from satellite observations' by Rankl et al.

The authors want to thank both reviewers for their careful reading of the manuscript. The comments were very useful and helped to improve the manuscript substantially. Large parts of the manuscript have been re-structured following the suggestions given by Ted Scambos. More methodological aspects brought up by Reinhard Drews have been addressed extensively in the revised version of the manuscript. In the following, all comments are addressed specifically and changes in the manuscript indicated. We hope, both reviewers support the changes made in the revised manuscript.

Comments by Ted Scambos:

Using a time-series of InSAR and speckle-tracked radar images of velocity, Rankl et al. present very good detailed study of the events occurring on the Wilkins Ice Shelf spanning the 1990s and through the series of major calvings and disintegrations occurring in 2008 and 2009. The focus of the paper is on ice flow and strain rates as the ice shelf evolves. This analysis of events provide insight into how stresses are transferred within ice shelves, and illustrate the power of good sequential ice velocity data in diagnosing causality for riftings and calvings.

In general, the writing could be tighter. There are some odd constructions for an English first-language reader, although the meaning is clear enough. But some work on the text could probably reduce the length by 10% and make it an easier, more efficient read. In reading it, I was interested by the main data figures (Fig2, 3, and 4) but found the discussion hard to follow because of the detail – all quite accurate, but it seemed to go slowly through this part when it could have been more interesting.
We did restructure the discussion following the reviewer's suggestion below.

My main comment concerns the interpretations of Figure 2 and 3 and 4 – the data look very good, and they provide a clear story – although I see you are cautioning about data quality in slow-moving areas. What is striking is the abrupt shift in the pattern after the calving and disintegrations of Feb-March, and especially after July, 2008 – this shows that the middle section of the ice bridge was an important buttress, and that the last ice bridge whisker was already nearly detached at the northern end (see Fig 5 in Braun et al. 2009 and Fig2 in Scambos et al. 2009 – the connection to Charcot Is. is rifted and sheared prior to the removal of the central ice bridge piece). With the loss of the middle ice bridge section, strong extensional stress is present just north of the Vere ice rise, and the ice soon rifts away ..
Sections 4.1 and 4.2 work through the data in the figures slowly. . . it would be more emphatice and clear to introduce the three figures briefly (just say what they are) and then discuss the evolution of the fractures and strain rates in a more story-like fashion. Readers would retain the events and significance better.

Or perhaps open with a) brief description of the data shown in the figures, and caveats, then, b) an overview 'story' of how events proceeded and the major fractures and shifts in strain patterns, and then c) perhaps some kind of review of the details captured by the Fig3 and 4 data that you are discussing on Page 6 and 7.
We thank the reviewer for this useful suggestion. We followed the reviewer's suggestion to split the discussion into 3 parts. The changes have certainly facilitated the readability of the manuscript and highlight the main results more succinctly.

I think the data make the sudden rearrangement the highlight of the paper; they underscore the relative lack of importance of the easternmost section of the ice bridge (or, if you like, the importance of the middle section.)

Overall, I think the manuscript is nearly publishable as it is, but would benefit and be more likely to be remembered and cited with another round of editing with respect to telling the story more clearly and succinctly. The conclusions have this kind of 'voice'.
The conclusions have been restructured.

P2L1 – in several papers, I've been trying to reserve this word for the kind of fine-scale rapid calving that was observed on Larsen B in January - March 2002 and Wilkins in Feb29-March8 2008. Please use the word 'collapse' here, since the ice shelf instability caused by the loss of the compressive arch might simply result in a series of large-scale calvings spanning months or even years, and not a true 'disintegration'.
We thank the reviewer for this helpful advice. The sentence has been changed accordingly.

P3L13 SNR: This needs a bit of unpacking – what you mean is a correlation peak height that is less than 4 times the mean correlation away from the peak. 'Signal' to 'noise' is a bit obscure here.
The reviewer is right with his explanation here, however, the term signal-to-noise ratio is commonly used when measuring the confidence of the offset estimates derived from intensity offset tracking (Seehaus et al., 2015; Strozzi et al., 2002; Werner et al., 2005). Thus, we would like to keep this terminology.
P5L33-34 Yes, extensional strain, but once the rift had formed in July 2007, almost all of the 'strain' would be taken up by the rift widening. It's what the strain rate was prior to the new rift (which, agreed, would have been formed by the stress build-up).
This remark of the reviewer is very subtle as it refers somehow to the transient stress evolution during fracture opening. Certainly, the stress field evolves as rifts open. This is difficult to trace with displacement fields inferred from consecutive image pairs acquired with a time lag of many days or even months. These displacements are highly averaged, while the rearrangement might have taken place on much shorter time-scales. We added this notion to the text when introducing the results.
P7L3 – '. . .it is obvious . . .. ' this phrase is odd, the block might have just calved away intact?
This ambiguous formulation was removed during rewriting the entire section following the main reviewer comments.
P7L8-25 I find this section somewhat of a difficult read – too tentative, to qualified; there's a basic story from the data, but it's obscured by nuance here. For example, L19-21, the ice bridge has a stabilizing effect, yes, and that places it under compressive strain along its axis, thus leading to, not failing to prevent, its eventual collapse - ?
Also, this paragraph was rewritten more clearly and succinctly during re-organization of the result section.
Fig3 and Fig4 – there is a white (fig3) and red (fig4) dot near the northeastern corner of the ice bridge – what does that signify? Please describe it in the captions.
The red/white dots mark an ice rise at the northeastern corner of the ice bridge. In the revised figures we removed the dots, since this information is not relevant for the analysis.

Please also note the supplement to this comment:
We thank reviewer for his helpful comments. The manuscript has been adapted accordingly.

References:
Seehaus, T., Marinsek, S., Helm, V., Skvarca, P. and Braun, M.: Changes in ice dynamics, elevation and mass discharge of Dinsmoor–Bombardier–Edgeworth glacier system, Antarctic Peninsula, Earth Planet. Sci. Lett., 427, 125–135, 2015.

Strozzi, T., Luckman, A., Murray, T., Wegmuller, U. and Werner, C. .: Glacier motion estimation using SAR offset-tracking procedures, Geosci. Remote Sens. IEEE Trans. On, 40(11), 2384–2391, 2002.

Werner, C., Wegmuller, U., Strozzi, T. and Wiesmann, A.: Precision estimation of local offsets between pairs of SAR SLCs and detected SAR images, in Proceedings. 2005 IEEE International Geoscience and Remote Sensing Symposium, 2005. IGARSS'05., vol. 7, pp. 4803–4805, IEEE., 2005.

Dynamic changes on Wilkins Ice Shelf during the 2006-2009 retreat derived from satellite observations

Melanie Rankl[1], Johannes Jakob Fürst[1], Angelika Humbert[2/3], Matthias Holger Braun[1]

[1]Friedrich-Alexander Universität Erlangen-Nürnberg, Institute of Geography, 91058 Erlangen, Germany
[2]Alfred Wegener Institute, Helmholtz Centre for Polar and Marine Research, Glaciology Section, 27568 Bremerhaven, Germany
[3]University of Bremen, Department of Geosciences, 28359 Bremen, Germany

Correspondence to: Melanie Rankl (melanie.rankl@fau.de~~)~~), Johannes Fürst (johannes.fuerst@fau.de)

Abstract. ~~Ice shelves serve as~~ The vast ice shelves around Antarctica can provide significant restraint to the outflow from adjacent tributary glaciers. This important ~~buttresses for upstream areas. Several large~~buttressing effect became apparent in the last decades, when outlet glaciers accelerated considerably after several ice shelves were lost on the Antarctic Peninsula~~ have disintegrated or retreated, which implied dynamic consequences for upstream ice.~~. The present study aims to assess dynamic changes on Wilkins Ice Shelf during ~~multi-stage~~a series of ice-front retreat ~~in the last decade. A total area of~~ and partial collapse between early 2008 and 2009. The total ice-shelf area lost in these events was 2135 ± 75 km² ~~was lost in the period 2008-2009.~~ (~15% of the ice-shelf area in respect to 2007). The present study uses time-series of Synthetic Aperture Radar (SAR) satellite observations (1994/96, 2006-2010) in order to derive variations in ~~multi-temporal~~ surface-flow speed from intensity-offset tracking~~ methods~~. Spatial patterns of horizontal strain-rate, stress and stress~~ components were inferred~~ flow angle distributions are determined during different ice-front retreat stages. ~~These fields are used~~Prior to ~~explain~~ the ~~different~~final break-up ~~stages and to evaluate the ice-shelf stability. For this purpose, we apply criteria which~~of the ice bridge in 2008, a strong speed-up is observed, which transmits into the derived quantities. Most helpful for identifying areas of buttressing or areas prone to fracturing were ~~forwarded to explain and assess past ice-shelf~~in-flow and first principal strain-rates as well as principal stress components. Further propagation can be explained as the first principal components of strain-rates and stresses exceed documented threshold values. A positive sign of the second principal stress is found to be another scale-free indicator for ice-shelf areas, where fractures preferentially open. Second principal strain-rates are found to be rather insensitive to ice-front retreat or fracturing, while changes seen in stress-flow angles lack a defined threshold for comparison.

1 Introduction

~~Antarctic~~During the last few decades several vast floating ice shelves ~~are sensitive indicators for global climate change (~~have been lost (Cook and Vaughan~~ and~~, 2010; Doake~~, 1996). Ice-shelf collapse or break-up led to tributary-glacier acceleration~~ and ~~dynamic~~Vaughan, 1991; Rott et al., 2002; Scambos et al., 2003, 2000), which entailed significant speed-up and thinning of previously restrained outlet glaciers (Berthier et al., 2012; Rignot, 2004; Scambos, 2004). The reason is that ice shelves restrain the outflow from tributary glaciers~~,~~ (Dupont et al., 2005), thus they serve as natural buttresses (De Angelis and Skvarca, 2003; Khazendar et al., 2015; Rott et al., 2002; Scambos et al., 2014). ~~Outflow increase becomes sea-level relevant when it reaches a key upstream location, the grounding line (Rignot, 2004; Shuman et al., 2011). This line pins down the location where ice becomes afloat on its general way towards the ocean.~~ On the Antarctic Peninsula (AP), 12 major ice shelves have either disintegrated or significantly retreated (Cook and Vaughan, 2010; Doake and Vaughan, 1991; Rott et al., 2002; Scambos et al., 2003, 2000). In addition, many of these ice shelves experienced important thinning over the past two decades (Fricker and Padman, 2012; Paolo et al., 2015; Wouters et al., 2015; Zwally et al., 2005). Ice shelves along the western coast of the AP exhibit thinning rates that are often twice as high as those on the eastern side (e.g., Larsen Ice Shelf) (Paolo et al., 2015). ~~87~~ Over 85% of the tributary glaciers showed retreating tongues (Cook, 2005). Reasons for this regionally concentrated ice shelf recession ~~or break-up~~ are manifold. Explanations range from a warming atmosphere (O'Donnell et al., 2011; Steig et al., 2009; Vaughan et al., 2003), to a reduction in sea-ice coverage on the western side of the AP (Stammerjohn et al., 2008), to rising ocean temperatures on the Bellingshausen Sea continental shelf (Martinson et al., 2008; Meredith and King, 2005) and to warming deep waters in the Weddell Sea (Robertson et al., 2002).

As it is long known that ice shelves serve as natural buttresses (De Angelis and Skvarca, 2003; Khazendar et al., 2015; Rott et al., 2002; Scambos et al., 2014), there were regular attempts to assess their structural stability under ice-front recession. A first criterion was formulated after the final collapse of Larsen A~~, within only one week,~~ and during the subsequent gradual recession of Larsen B. Doake et al. (1998) inferred ~~all horizontal~~ the two principal strain-rate components~~.~~ in horizontal direction. The ~~sign of the~~ smaller ~~eigenvalue of the~~ second principal strain-rate ~~tensor was then used to determine a line, downstream of which the ice-flow regime is exclusively~~differentiates areas of purely extensive ~~(all eigenvalues positive). This~~ice flow from more constrained regions. A 'compressive arch' was forwarded ~~as~~to delineate a threshold ~~contour for frontal recession,~~ line, beyond which ice shelves are expected to ultimately ~~disintegrate~~collapse. In the meantime, ice-flow models were successfully applied to get a more comprehensive description, including the stress distribution. Studying Larsen C ice shelf, Kulessa et al. (2014) proposed that ice-shelf stability should be assessed from the stress-flow angles~~. It is~~, i.e., the angle between the ice-flow direction and the first principal stress ~~direction~~. When the the two fields align and the angle tends to zero, fracture opening rates were considered to maximize. If angles are small near ~~the~~an ice front, ~~this~~the ice-shelf geometry would be considered ~~a less~~not very stable ~~state~~.

Also relying on the stress regime within the ice, Fürst et al. (2016) quantified the maximum buttressing potential of all ice shelves in Antarctica. Though not addressing the stability issue, they could show that ~13% of all floating ice is dynamically not relevant. Once ice-front recession exceeds this passive shelf-ice area, dynamic consequences are expected. For ice shelves in the Bellingshausen Sea, only a small 5%-fraction can still be removed without dynamic implications.

The aim of this study is to assess changes in the dynamic state of Wilkins Ice Shelf (WIS) ~~under~~during the multi-stage break-up during the last decade. For this purpose, ice-velocity maps are inferred from radar satellite observations in 1994/96 and from 2006-2010. From these maps, we ~~infer~~derive time-series of strain-rates~~ and~~, the principal stress distribution~~. These fields will then help to explain~~ and stress-flow angles. Changes in these time-series are discussed during the different collapse stages on WIS, which allows ~~us to assess the~~a first assessment of invoked stability criteria ~~forwarded in the literature~~ (Doake et al., 1998; Fürst et al., 2016; Kulessa et al., 2014).

2 Study area

WIS is located at the south-western part of the AP covering an area of 10,150 km² in April 2015. The ice shelf is confined by Alexander, Rothschild and Latady Island. Mass gain at WIS is dominated by surface accumulation (Vaughan et al., 1993). Further contribution of mass originates from the main in-flow ~~from~~of Lewis Snowfield south-west of the ice shelf. Contribution of mass from Gilbert Glacier and two inlets, called Schubert and Haydn inlets, is highly ~~restraint~~restrained by prominent ice rises (e.g. Dorsey Island).

During the last decades, WIS has undergone significant dynamic changes: Surface lowering of in total -4.95 ± 0.21 m between 1978 and 2008 at the southern WIS (Fig. 1) was found to be the largest for all AP ice shelves (Fricker and Padman, 2012). In recent years (2000-2008), however, thinning rates were less negative or even slightly positive at the northern WIS (Paolo et al., 2015). Average thickness changes at WIS ~~account for~~were -0.62 ± 0.12 m a^{-1} for the period 1994-2012 derived from radar altimetry and were attributed to basal melting (Paolo et al., 2015). Basal melt rates of WIS were estimated by several authors: Holland et al. (2010) found 0.66 m a^{-1} averaged over the period 1979 to 2007, Padman et al. (2012) inferred rates of 1.3 ± 0.4 m a^{-1} during 1992-2008, while Rignot et al. (2013) derived 2003-2008 average rates of 1.5 ± 1 m a^{-1}.

In addition, the WIS underwent major ice-front retreat ~~has been detected~~ (Braun et al., 2009; Scambos et al., 2009, 2000). Based on the analysis of ~~multi-temporal~~time-series of satellite imagery and historic maps, ~~several~~numerous break-up stages were quantified (Arigony-Neto et al., 2014). Several causes for break-up at WIS were proposed in the literature: fracture formation due to bending stresses in combination with surface melt or brine infiltration (Scambos et al., 2009), transoceanic infragravity waves which induce fractures at Antarctic ice shelves (Bromirski et al., 2010) and break-up due to bending stresses caused by enhanced basal melt (Braun and Humbert, 2009; Humbert et al., 2010). Continuous ice-front retreat led to the formation of a remnant ice connection between Latady and Charcot Island at the western WIS (ice bridge in Fig. 1a), which collapsed in April 2009. Braun et al. (2009) also documented the development of fractures and rifts as well as the role of ice rises in the break-up processes on WIS. Between 28/29 February and 30/31 May 2008, an area of 585 km² broke-off narrowing the connection between these two confining islands (Braun et al., 2009). In June/July 2008, an area of 1220 ± 75 km² (~8% of the ice-shelf area in respect to 2007) was lost at the eastern side of this ice bridge (Fig. 1a), ~~meaning~~implying further weakening ~~of it~~ (Humbert and Braun, 2008). Braun and Humbert (2009) found highly variable ice thicknesses (~250-170 m) along the ice bridge implying important buoyancy differences. The break-up events in May and June/July 2008 have demonstrated that such events can occur in austral winter (Braun et al., 2009). This contradicts previous assumptions that ice-shelf break-up mainly depends on summer surface melt ponds (Doake and Vaughan, 1991; MacAyeal et al., 2003; Scambos et al., ~~2009~~2000). In early April 2009, the final ice-bridge collapse corresponded to an area loss of 330 km². More than 100 tabular icebergs calved off. Many of these icebergs capsized, releasing an energy of >125 x 10^{6} J (Humbert et al., 2010). After the collapse of the ice bridge, small-size calving events occurred, which primarily took place along the south-west ice front between Latady Island and Lewis Snowfield.

3 Material and Methods

~~3.1 SAR intensity offset tracking~~

3.1 Surface velocities

Surface velocities of the ice shelf and its tributary glaciers were derived from SAR (Synthetic Aperture Radar) intensity-offset tracking (Strozzi et al., 2002) using repeat ALOS PALSAR (46 day time interval) ~~and ERS-1/-2 (35 day time interval) SAR~~ Single Look Complex (SLC) image pairs (Table S1). ~~This~~Results in March 1994/96 were taken from InSAR (Interferometric Synthetic Aperture Radar) derived surface flow presented in Braun et al. (2009) and from ERS-1/-2 (35 day time interval) intensity-offset tracking. The latter technique cross-correlates the backscatter intensity pattern of a pair of SAR images of different acquisitions dates. For this purpose, small image patches are shifted over the entire image (Table 1) and for each patch, the maximum of the 2-D cross-correlation function yields the image offsets in range and azimuth directions. If coherence between both image patches is retained, the speckle pattern is additionally correlated. Offsets of minor confidence were rejected based on a signal-to-noise-ratio (SNR ≤ 4). The processing was performed using Gamma Remote Sensing software~~.~~ (Werner et al., 2000). Geocoding of the final range and azimuth offsets from SAR to map geometry was based on the WGS84 ellipsoid. The output spatial resolution was set to 50x50 m, which is also true for the derived quantities in 3.2.

The method relies on surface patterns, which are identifiable in both images. However, co-registration and intensity-offset tracking performed on single scenes of the nearly structure-less ice shelves was ~~hardly~~rarely successful. Therefore, single scenes ~~along the respective relative orbits~~ were concatenated along-track (Fig. S1). Additionally, we used a binary mask of non-moving (e.g., ice rises, bedrock) and moving areas (ice shelf, tributary glaciers, sea) to perform co-registration on stable areas only (Fig. S1). In a post-processing step, the ~~surface~~ flow ~~was~~magnitude and direction were filtered using the approach described in Burgess et al. (2012). By using a 5 x 5 pixel ~~median filter and a threshold discarding flow~~moving window approach, displacement vectors were discarded iteratively when deviating more than 30% from ~~a reference direction applied.~~ the median length of the window's centre vector or when deviating from a predefined orientation of the centre vector (thresholds 20°, 18° and 12°).

For each year, several displacement fields ~~of different relative orbits~~ were mosaicked. ~~Results in 1994/96 were taken from InSAR (Interferometric Synthetic Aperture Radar) derived surface flow presented in Braun et al. (2009) and from ERS-1/-2 intensity tracking. For each absolute flow field between 2006 and 2010, a mosaic of three to four relative ALOS PALSAR orbits represent the surface flow for the respective time period, mostly in austral summer (August/September to October/November in 2007-2010, Table S1). Ice flow in 2006 covers the period mid-May to mid-June. Due to the time difference between image acquisitions, the~~The mosaicked surface flow shows slight deviations in the flow magnitude ~~at~~along the boundaries of each ~~relative orbit. Hence, flow~~satellite flight path. These offsets might be due to short-term variations of ice flow between image acquisitions, processing artefacts or due to varying co-registration accuracies related to the restricted availability of non-moving areas in each scene. The magnitude of these offsets is non-linear and ranges between ~3 and 18 m yr^{-1} on the main ice-shelf area. Of course, the offsets are larger close to the ice front, where the displacement fields capture the short-term motion of the ice mélange. The derived flow fields were not corrected for these non-linear offsets, however, the estimated co-registration accuracy in Table 2 accounts for these deviations (see below). Flow differences for 2007/2008 and 2008/2009 were calculated ~~solely~~ for the south-western ~~orbit in order to show results independent from overlapping velocity results.~~ part of the ice shelf only, since this part reveals the most important dynamic changes.

The estimation of errors in the derived velocity fields was done as described in McNabb et al. (2012) and in Seehaus et al. (2015). For each velocity field a value based on the accuracy of the co-registration (σ_v^C) was calculated and a second value (σ_v^T) described uncertainties involved in the intensity-offset tracking algorithm (Table 2). Further error contribution related to the orbital information of the image acquisitions or the atmospheric influence are still difficult to quantify. The magnitude of the term σ_v^C was derived from the median of the velocities over non-moving areas (based on up to 25,000 samples per image pair), e.g., ice rises, bedrock, where zero ice motion is assumed. The error estimation over non-moving ground is a standard procedures when using intensity-offset tracking for ice velocity determination (e.g., Burgess et al., 2012; McNabb et al., 2012; Quincey et al., 2009, 2011; Seehaus et al., 2015). ~~was calculated and a second value described uncertainties involved in the intensity tracking algorithm (Table S2).~~Since no additional calibration of the derived offset fields over stable ground has been undertaken, the term σ_v^C captures all errors related to the co-registration procedure. The second term σ_v^T describes uncertainties related to the intensity-tracking algorithm, the spatial resolution and time interval between image acquisitions. It is calculated using

$$\sigma_v^T = \frac{C\Delta x}{z\Delta t} \qquad \text{(Seehaus et al., 2015).} \qquad (1)$$

C describes the uncertainty of the tracking algorithm (C=0.4), Δx the image resolution in ground range, z the oversampling factor used in the tracking process and Δt the time period between image acquisitions. The final error estimate σ_v is derived from the sum of both terms σ_v^C and σ_v^T (Table 2).

When calculating the strain-rate and stress components from the displacement fields (see 3.2), a wavelike pattern emerges in 2006, 2008 and 2009, which dominates in areas where flow speeds are small. This pattern was detected in comparable studies calculating surface velocities from intensity-offset tracking (Joughin, 2002; Nagler et al., 2015). It was attributed to fluctuations in the polar ionospheric electron density and may affect the phase measurement of a SAR sensor, but also the correct mapping of the azimuth pixels' position (Gray et al., 2000). This effect is found to be larger for L-band than for C-band acquisitions. The wavelength of this pattern in L-band frequencies was scaled to 5-10 km (Gray et al., 2000), which is also true for the pattern visible in Figures 3 and 4 in the present study. A smoothing of this pattern by averaging several flow fields over multiple acquisitions as proposed in Nagler et al. (2015) is impossible on WIS due to lack of further, suitable image pairs. Another study found variations in the tropospheric water content influencing the measured path delay with InSAR (Drews et al., 2009). However, this effect was restricted to C-band InSAR (Williams et al., 1998) and no influence on the image intensity is known. Hence, ionospheric disturbances remain a likely explanation for the detected wavelike pattern in this study. However, as the pattern has some link to the structure of the ice shelf and is persistent over years, we cannot rule out completely that it is a real feature of the displacement field.

3.2 Stress tensor and strain-rates

In order to infer the components of the stress tensor associated with a flow field, a constitutive equation is required. In glaciology, ice is typically described as being a non-Newtonian fluid with a viscosity η depending on temperature and effective strain-rate. In its most general form, the constitutive equation for the deviatoric stress τ_{ij} can be written as follows:

$$\tau_{ij} = 2\eta \cdot \dot{\varepsilon}_{ij} \qquad (~~1~~2)$$

Here, $\dot{\boldsymbol{\varepsilon}}$ is the strain-rate tensor, which holds information on spatial derivatives of the horizontal velocity field:

$$\dot{\varepsilon}_{ij} = \frac{1}{2}\left(\frac{\partial u_i}{\partial x_j} + \frac{\partial u_j}{\partial x_i}\right) \qquad (~~2~~3)$$

The strain-rate tensor describes how much the ice is deformed at a certain location and its horizontal components can be inferred from surface velocities. For the purpose of understanding the changes in the stress regime due to the break-up events, it is of particular importance to look at strain-rates and not velocity fields. Velocity fields are derived by measuring displacements of features assuming that the features themselves do not change. In case of opening of a rift, the feature is often a rift face or a crack front, and both change over time. Thus, the interpretation of the displacement field as a flow velocity can only be done in case there is no rift opening. Otherwise, the displacement due to opening of a rift and the creep of ice are superimposed in the velocity field. Strain-rates, however, overcome this flaw, as they are spatial derivatives.

The ice viscosity ~~then~~ determines how strain-rates translate into deviatoric stresses τ_{ij}. Stress deviators are linked to the full Cauchy stress $\boldsymbol{\sigma}$ by adding the isometric pressure.

$$\tau_{ij} = \sigma_{ij} - \frac{1}{3}\delta_{ij}\sum_k \sigma_{kk}$$ ~~(Pattyn, 2003) (3~~

(Cuffey and Paterson, 2010) (4)

At the ice-shelf surface (denoted as superscript s in the following), where satellite data ~~is~~was acquired, the relation between deviatoric and full stresses simplifies to:

$$\sigma_{xx}^s = 2\tau_{xx}^s + \tau_{yy}^s \qquad (~~4~~5)$$

$$\sigma_{yy}^{s} = \tau_{xx}^{s} + 2\tau_{yy}^{s} \quad (~~5~~6)$$

This assumes that ~~horizontal~~ bridging effects are negligible near the ice surface. ~~At~~Given the fact that we observe the horizontal velocities at the ice-shelf surface, ~~the horizontal Cauchy~~ we can compute from (5) and (6) the stress components ~~are a sum of the horizontal deviatoric stress components, which in turn can be inferred from the strain fields. Therefore our discussion is limited to the surface conditions of~~at the ice-shelf surface. In the following, however, we will ~~often~~ omit ~~to specify~~specifying this limitation and simply speak of strain and stress conditions.

~~In addition, the~~The viscous response of an ice body is ~~not necessarily~~ non-linear and depends itself on the strain regime:

$$\eta = \frac{1}{2} m A^{-1/n} \cdot \dot{\varepsilon}_{e}^{(1-n)/n} \quad (~~6~~7)$$

Here, $\dot{\varepsilon}_{e}^{2} = \frac{1}{2}[$~~$(tr(\dot{\varepsilon}))^2 - (tr(\dot{\varepsilon}^2))$~~$](\Sigma_i \dot{\varepsilon}_{ii})^2 - \Sigma_i(\dot{\varepsilon}_{ii}^2)]$ is the second invariant of the strain-rate tensor. We assume isotropic material properties and a flow exponent of $n = 3$. A is the rate factor, which determines the readiness of the viscous material to deform under a given stress (Van der Veen, 2013). For WIS, we assume a constant rate factor A of 1.7 x 10^{-24} Pa^{-3} s^{-1} (Cuffey and Paterson, 2010) corresponding to near-temperate ice of about -2° C as observed in this area (Braun et al., 2009). The rate factor is ~~generally~~ a function of ice temperature and microscopic water content and consequently ~~varies on ice-shelf scales~~can show some spatial variability. The enhancement factor m is assumed constant and set to 1. In general, m is, however, a function of grain size, impurities, damage degree and other variables (Cuffey and Paterson, 2010, p. 71). These additional factors are difficult to account for and are therefore not reflected in the subsequently presented stress fields. ~~However, the zero stress line remains unaffected by this scaling issue.~~

Strain and stress components are real and~~, by construction, the strain rate and stress~~ respective tensors are symmetric~~. Therefore~~ which ultimately reflects the conservation of angular momentum in continuum mechanics. As a consequence, all eigenvalues are ~~also~~ real.~~ Moreover, we order the two eigenvalues for each tensor by size. In general, the larger eigenvalue of these tensors is referred to as the first principal component (Doake et al., 1998; Kulessa et al., 2014).~~ First and second principal components span the range of minimal and maximal extensive or compressive strain-rates or stress occurring at the ice surface~~.~~ (Gross et al., 2009). The first principal strain-rate gives maximal extension rates and is therefore of interest to define a crevasse initiation or material failure criteria (Benn et al., 2007; ~~see~~ Vaughan, 1993). ~~Observed~~

The strain and stresses components in this study will be used in two regards: (i) for assessing the change in them after break-up events and (ii) to assess which area of the ice shelf might reach a critical limit and be prone to new crack initiation. Suggested threshold -strain-rates for fracture initiation span a wide range from 0.01 a^{-1} (2.~~7E~~$7 \cdot 10^{-5}$ day^{-1}) on Greenland (Meier, 1958) to 0.004 a^{-1} (1.~~0E~~$0 \cdot 10^{-5}$ day^{-1}) on White Glacier, Canada (Hambrey and Müller, 1978). To describe damage initiation within an ice body, Krug et al. (2014) used a threshold criterion for the first principal stress component. In terms of stresses, inferred thresholds range from 90 to 320 kPa (Vaughan, 1993). The Hayhurst rupture criterion defines a stress threshold of 330 kPa for fracture initiation (Pralong et al., 2006). Second principal surface stress, however, was recognized to be important in terms of ice-shelf stability (Doake et al., 1998) or, more general, to assess and quantify the dynamic susceptibility of ice shelves (Fürst et al., 2016).

4 ~~Ice~~ Results

In the following, dynamic ~~changes~~consequences of the successive retreat stages of WIS are analysed on the basis of multi-temporal maps of surface velocities, strain-rates, principal surface stresses and the stress-flow angle criterion (Figs. 2-4). First, we will give a short overview of the figures stating the importance and caveats of the presented velocity data and the derived quantities (Sect.

4.1). Then, we will use all fields to analyse the dynamic re-organisation of the ice shelf during the different retreat stages (Sect. 4.2). Finally, we will investigate which quantities are most suitable for identifying ice-shelf instability (Sect. 4.3).

4.1 Results Overview

We present a unique sequence of multi-temporal surface velocity maps for WIS spanning the period 1994/96 to 2010 (Figs. 2 & 3). During all years, the ice shelf is mainly fed by Gilbert Glacier, Haydn and Schubert inlets as well as directly from the Lewis Snowfield. For the grounded part of Gilbert Glacier, surface velocities readily exceed 300 m yr^{-1}. Yet, once the grounding line is passed, velocity magnitudes decrease rather quickly. Inflow from Gilbert Glacier and Haydn inlet is prominently restrained by Dorsey Island. Further west, additional restraint is provided by the Petrie and Vere ice rises as well as by Latady Island. This initial deceleration is characteristic for all major outlet glaciers draining into WIS and it illustrates that ice-shelf flow is highly constrained by the geometric setting (islands, ice rises and pinning points). Dependent on the consecutive image pair (Table 2), the velocity error associated to the intensity-offset tracking method falls into a range between 25 to 100 m yr^{-1}. In 1994/96, ice-shelf velocities show comparable magnitudes (Fig. 2a). Break-up at WIS was analysed using multi-temporal surface flow in 1994/96 and between 2006 and 2010 (Fig. 2). Figure 3 shows the period between 2006 and 2009 in more detail, when the ice bridge gradually collapsed. The general picture of surface flow shows prominent inflow from Gilbert Glacier, Haydn and Schubert inlets, and directly from Lewis Snowfield over all years 1994/96 and 2006-2010 (Fig. 2), where flow In more recent years, velocities are found to be higher and their magnitudes are thus, relatively more reliable. The 2006/2007 acceleration shows a meaningful pattern with largest values near the northern-western ice front. The relatively high error value associated with the velocity fields has, however, to be considered when interpreting all derived quantities as these rely on sensitive spatial velocity differences. Despite the velocity error, offset tracking produces velocity fields representative for time periods covering many days or even months (Table 2). When we interpret and discuss these fields, it is essential to keep in mind that values might represent an average displacement and that we cannot discern between sudden or gradual flow re-organisation.

The first derived quantities are the strain-rates can exceed 1.5 m day^{-1}. The inflow is, however, restrained and deviated for instance by Dorsey Island or by the ice rises in front of Haydn and Schubert inlets.

The entire ice shelf showed very small velocities in March 1994/96. Slightly higher surface motion was encountered in the south-west, originating from Lewis Snowfield as well as near the ice front at Charcot Island after the 1993 break-up event (remnant icebergs are still visible in the backscatter SAR image in Fig. (Fig. 3). Positive values indicate 2a). Between February and June 1998, a large double fracture formed almost parallel to the western ice front of the ice bridge between Latady and Charcot Island (green line in Fig. 3a). In July 2007, surface flow on the ice bridge increased due to the formation of the second longitudinal fracture-pair (purple line in Fig. 3e). This acceleration was followed by major ice loss on the western and south-eastern ice bridge between February and July 2008 (Braun and Humbert, 2009; Humbert et al., 2010). A total area of 1805 ± 75 km² was lost. The consecutive acceleration was most expressed on the ice bridge (up to ~ 0.8 m day^{-1} at the narrowest part), but did certainly reach as far upstream as to the Petrie Ice Rises (Fig. 2g). Upstream of this region, acceleration is somewhat lower. The north-western part of the ice bridge remained rather stagnant, still experiencing and transmitting the buttressing from Charcot Island (Fig. 3i). The narrow remainder of the ice bridge finally collapsed in April 2009 and an area of 330 km² broke off (Humbert et al., 2010). This final event caused almost no additional upstream acceleration (Fig. 2h). This suggests that the lost ice-shelf portion did not transmit or provide an important restraint to the central ice-shelf unit. In 2010, results from feature tracking were unavailable for some parts of the WIS and the coverage was incomplete (Fig. 2f). Yet, from the covered areas of the ice shelf, we are confident that ice flow did not change significantly between 2009 and 2010 (Fig. 2e, f). In addition, the ice-front position remained stable during this period (Fig. 2f).

From the strain-rate tensor, we inferred the component pointing in flow direction. This in-flow strain rate gives an indication on whether the extensive flow regime is extensive or , while negative values imply compressive along streamlines. Yet, the qualityflow. The reliability of the in-flowthese strain rate rates is highly dependent on the reliabilityquality of the inferred flow directions. Very lowmagnitude and direction. Relative errors become dominant in areas where flow speeds, as found on the main ice shelf in 2006 and 2007, are more susceptible to errors (Fig. 3a, e). Thus, for the interpretation of in-flow strain-rates are small. To avoid misinterpretation in such areas, we willmostly limit the following discussion to areas showing considerable motion. The (≥ 0.05 m day^{-1} or 20 m yr^{-1}). Additionally, we calculated values at each point in a local coordinate system with the two axis aligned parallel and perpendicular to the local flow direction. In this way, we can determine the strain-rate in flow direction. Where ice flow is restrained by obstacles, such as ice rises, island and other pinning points, this strain-rate component is negative and thus, compressive in all years 2006-2009, where the ice flow is blocked by an obstacle, e.g., upstream of the Petrie Ice Rises. (Fig. 3b, f, j, n; compressive strain rates correspond to negative values). Compressive strain rates also prevail close to). Additional inflow originating from Latady Island, where a slight inflow is visible (Fig. leads to compressive strain-rates further south (Fig. 3b, f, j, n). Extension and thus positive strain rates dominate in 2006 and 2007 along the ice bridge (Fig. 3b, f; red values indicate extensive strain). In 2008, most parts of the ice shelf show extensive flow, merely buttressed by the Petrie Ice Rises and Latady Island (Fig. 3j). In-flow strain rates of opposite sign on each side of the narrowest part of the ice bridge in 2008 explain the formation of an initial crack and why the ice bridge failed there. The prevailing atmospheric circulation pushed the brittle ice mélange westward, which was forwarded as a reason for why the bridge yielded in this direction (Humbert et al., 2010).

The first principal strain rate gives the maximum stress value (All strain-rate components are elevated, where Fig. 3c, g, k, o). It is positive all over the ice shelf in all years, which means that the ice experiences extensive stress in a certain direction. Local maxima, i.e. maximum extension, occur on the lee side of ice rises and where fractures formed on the ice bridge in 2007 (Fig. 3g) and alongside Vere Ice Rise in 2008 (Fig. 3k).

The second principal strain-rate component is negative in all years (Fig. 3, lower panels). This implies that the flow regime of WIS has a compressive component almost everywhere. As ice flow accelerates from 2006have formed or continue to 2008, the second principal strain rate becomes less negative (Fig. 3d, h, l). After the final collapse of the ice bridge, this strain-rate component drops down again to pre-collapse values near the ice front and close to Latady Island (Fig. 3p). open.

Based on the calculation of surface flow in 2006-2009 and the basic assumption ofderived strain-rates and by assuming a constant rate factor, principal stress fields were derived in order to assess the fundamental changes in the stress regime during the ice bridge break-up.surface-stress components were computed (Fig. 4). The first principal stress gives the highest extensive stress acting within the material. In all yearsBetween 2006- and 2009, first principal stresses are generally positive (Fig. 4a, d, g, j). Local maxima in these fields coincide with Values are often elevated nearby fractures. It is not surprising that theseMoreover, local maxima are often located at the tip of these fracturesfracture tips, where extensive forces are focused. In 2008 and 2009, however, a wave-like pattern becomes visible on the main part of the ice shelf (Fig. 4g, j). These artefacts cannot be explained by processes occurring in the ice, but might be inherent to the satellite data (e.g., ionospheric noise (Gray et al., 2000; Meyer et al., 2006) or might result from the tracking algorithm.

Theconcentrate. Away from the ice bridge, the second principal stress component is mostly negative. This illustrates that ice flow is largely constrained by the geometric setting. As the magnitude of the stress field scales with the rate-factor choice, the latter discussion mostly focusses on the pattern and sign changes in the second principal stress holds information on the smallest extensive or largest compressive stress acting within the ice. For positive values, the ice-shelf surface experiences an exclusively extensive stress regime. In 2006 and 2007, field. Both are robust even if a different rate factor was chosen. Sign changes would even persist for a compressive second principal stress regime prevails on WIS (Fig. 4b, e). During the formation of the second double fracture on the ice bridge in 2007 (purple line in Fig. 4d), this region turns fully extensive in terms of stresses as well as first principal strain rates (Figs. 3g & 4e). Without any compressive components, the ice bridge was destined to split in two and the western part collapsed soon thereafter. In 2008, ice flow increased and with it the second principle stress. In large areas previously showing negative values, the stress regime turned entirely extensive in 2008 (Fig. 4h). The only exceptions are the vicinity of ice rises and near Latady Island. One year later, the stress state has reverted back to the pre-acceleration state with a largely compressive second principal component (Fig. 4k).

Assessing ice-shelf stability on Larsen C, Kulessa et al. (2014) introduced a newspatially variable. They computed rate factor field. Finally, the angle between the ice flow direction and the first principal stress direction. is computed. This stress-flow angle was introduced by Kulessa et al. (2014) to assess the stability of the Larsen C Ice Shelf under consecutive ice-front recession. They argue that when the flow direction and the first principal stress direction align, fracture formation is facilitated. This stress-flow angle is consequently used as a criterion for ice-shelf stability, which we follow here for comparison. Low stress-flow angles indicate areas, which are more likely to suffer from break-up, whereas larger stress-flow angles, approaching 90°, indicate stable conditions (Jansen et al., 2015). Stress-flow angles on WIS are small, where fractures formed, e.g., on the ice bridge in 2007 or upstream the ice bridge, parallel to the northern ice front in 2008 (Fig. 4f, i). Stress-flow angles on the ice bridge, however, show higher values in 2008 (Fig. 4i).

4.2 Assessing the retreat stages

In this section, we want to investigate, which fields are more or less informative, when it comes to identifying weaknesses and predicting the next break-up stage.

In 2006, no field shows any indication that another fracture pair would open. Near the existing double fracture, which formed in 1998 (Fig. 3a) local maxima are discernible for in-flow strain rates (Fig. 3b) and the first and second principal stresses (Fig. 4a, b). The latter stress even turns positive. Neither the second principal strain rate nor the stress-flow angle shows a well imprinted trace of the already present fracture.

Turning to 2007, most fields reflect the opening of the new fracture pair on the ice bridge (Figs. 3 & 4). Only exception is the second principal strain rate (Fig. 3h). From the ice velocities, it is obvious that the western part of the ice bridge started to accelerate and will soon disintegrate. None of the derived fields allows such a clear distinction of the bridge sides. An explanation is that all other variables are derived from spatial derivatives of the flow field. Despite this distinction, the strain field in flow direction turned compressive along the old fracture pair on the eastern part of the bridge (Fig. 3f). In the principal stress components we can discern a local stress maxima (pure extension) on the southwestern trunk of the ice bridge (Fig. 4d, e), which could explain fracturation there.

Stress-flow angles show very small values on the north-western end of the bridge (Fig. 4f). Following the interpretation from Kulessa et al. (2014), fracture opening would be facilitated. In this area, first principal stress components are not particularly elevated (Fig. 4d). The stress-flow angle criteria is, however, the only measure that points out instable conditions all along the north-eastern ice front, which actually retreated afterwards. Low values along the south-western ice front might be an artefact from not well constrained flow directions (Fig. 4f).

By 2008, ice flow fundamentally changed both in terms of direction and magnitude. All measures reflect this important change. The in-flow strain rates show different flow regimes on each side of the narrowest part of the ice bridge: upstream extension vs. downstream compression (Fig. 3j). This explains the later failure position. No other field can make an as clear distinction here. The second principal strain rate gradually increased since 2006 but still remains mostly negative (Fig. 3l). Even if zero is not passed, the stability interpretation from Doake et al. (1998) would suggest reduced retreat susceptibility as compared to the previous stages. However, the ice bridge was lost afterwards. The stress-flow angles suggest a different interpretation of this state. High values dominate on the ice bridge, while all the rest of the north-eastern ice front shows small angles (Fig. 4i). The interpretation of these angles would suggest that the ice bridge has a stabilizing effect on the upper more susceptible areas. This deduced stabilization could however not prevent the consecutive collapse. In this case, the interpretation of stress-flow angles is therefore delicate. Both for the Doake criterion and the stress-flow angle, the ice-shelf might already have adopted a flow regime consistent with the post-collapse ice front. An interpretation of the field downstream of the latter ice front position might be futile. For both principal stress components (Fig. 4g, h), as well as for the in-flow strain rates (Fig. 3j), values are highly elevated along the fractures, which later became the new north-eastern ice-front position.

The state in 2009 points towards stable conditions on WIS reflected in all measures. To date, no further ice-front retreat occurred at the northern ice front.

4.3 Ice-shelf stability

From the above assessment, some of the presented measures emerge to be more or less applicable for assessing ice-shelf stability. The most intuitive measure for interpreting the retreat stages might be the in-flow strain rates (Fig. 3) and the principal stress components (Fig. 4). Sign changes and local maxima in these strain-rate fields could be exploited in this interpretation. The fist principal strain-rate component can be used to describe a crevasse opening threshold on ice shelves. Local strain-rate maxima on the ice bridge in 2007 (Fig. 3g) and perpendicular to the ice bridge in 2008 (Fig. 3k) reach maxima between ~5E-5 and 1.3E-4 day^{-1}. The narrowest part of the ice bridge holds maximum first principal strain rates of ~1.2E-4 day^{-1} in 2008. Threshold strain rates determined for crevasse opening on other glaciers (Hambrey and Müller, 1978; Meier, 1958) show comparable or even smaller values. Therefore, the latter fracturation and ice-shelf break-up can be explained.

For the interpretation of the second principal strain-rate component (Fig. 3, lowest panels), we want to follow Doake et al. (1998). They forwarded that when the ice front retreats/recedes beyond a certain isoline in this strain-rate component, the ice-shelf integrity is no longer granted and a destabilization is expected. The stress value associated to this isoline is suggested to be close to zero. Second principal strain rates are rather insensitive during the retreat stages of WIS. Values are generally negative and therefore suggest general recession.

The first principal stress component points out regions, where fractures are likely to open or propagate (Krug et al., 2014; Vaughan, 1993). On WIS the threshold between 90 and 320 kPa mentioned above (Vaughan, 1993) holds for the break-up events in 2007 and 2008 (Fig. 4d, g). In 2007, the first principal stress regime on the ice bridge exceeded ~200 kPa as well as in 2008, when fractures parallel to the ice front formed (Fig. 4d, g). Values were slightly lower at the narrowest part of the ice bridge, where the ice bridge collapse initiated (Fig. 4g). Yet, the magnitude of this field scales directly with the rate factor, hence, any threshold criteria inferred from observations has to be considered with caution.

The second principal stress component shows some advantage in this respect (Fig. 4b, e, h, k). For all retreat stages, we confirm that this stress field shows a change in sign to positive values in critical regions. Such sign changes are unaffected by the rate factor choice. Thus, we think that positive second principal stresses add substantially to a pure strain-rate interpretation.

~~The stress-flow angle on WIS is rather ambiguous (Fig. 4 lowest panels). Though some retreat stages can be explained, this is certainly not the case for others. In defence of this measure, we have to add that the~~Otherwise, ice fronts are considered rather stable. On Larsen C, they found large angles near the present ice front, but once an existing and continuously propagating rift would trigger the next major calving event, the ice-shelf stability might be reduced. On WIS, we confirm that stress-flow angles are indeed small in areas where fractures formed. The derivation of stress-flow angles shown in Kulessa et al. (2014) is based on modelled ice-shelf velocities, flow lines and stresses using a continuum-mechanical ice-flow model. In the present study, however, the angle is calculated from observations, which results in ~~high~~a higher spatial variability of the underlying ~~principal strain-rate directions.~~ quantities.

4.2 Retreat stages

In March 1994/96, we find a rather stagnant ice shelf with surface velocities below 0.2 m day^{-1} (70 m yr^{-1}) in most areas (Fig. 2a). Increased flow rates are visible downstream of Lewis Snowfield and Gilbert Glacier. Velocities increase up to 1 m day^{-1} along the northern ice front near Charcot Island, which is likely associated with the 1993 break-up event there (remnant icebergs are still visible in the backscatter SAR image of Fig. 2a). Even though the northern ice front retreated significantly until 2006, no significant speed-up is observed (Fig. 2b). All along the elongated ice bridge connecting to Charcot Island, two distinct flow branches are discernible by a small step in velocity magnitude. The western branch shows higher velocities, which indicates that it already experiences and transmits less buttressing from Charcot Island. The disconnection between these two flow branches has likely started between February and June 1998, when a double fracture (~45 km long, green line in Fig. 3a) formed parallel to the western ice front (Braun and Humbert, 2009). The fracture is imprinted in all derived quantities and is most pronounced in the in-flow and first principal strain-rate components as well as in the first principal stress component (Fig. 3b, c and 4a). For the second principal stress component, the fracture is highlighted by a sign change to positive values (a fully tensile stress regime), while most of the remaining ice shelf shows a partially compressive regime.

In July 2007, the western branch of the ice bridge further accelerated in response to the formation of a second, longitudinal fracture pair (~37 km in length, purple line in Fig. 3e, Braun et al., 2009). A clear distinction of the acceleration in two branches is possible, with more elevated values along the western side of the bridge (Fig. 3e). Most of the derived quantities change in reaction to the opening of the fracture pair. Stress and strain-rate components show increased values and often pronounced maxima, while the stress-flow angle tends to smaller values (Figs. 3f, g & 4d, e, f). From the in-flow strain-rates and the second principal stress we observe that a narrow region on the eastern branch shows very negative values indicating important compression. Away from the ice bridge, all fields remain similar to the 2006 situation, which implies that there is no clear indication for an imminent dynamic re-arrangement. Buttressing due to e.g., ice rises is well expressed in low values in principal stresses as well as in the in-flow and second principal strain-rates (Figs 3f, h & 4d, e).

Between February and July 2008, the western branch of the ice bridge broke-off and an area of 1805 ± 75 km² (~12% of the former ice-shelf area) was lost (Braun and Humbert, 2009; Humbert et al., 2010; Scambos et al., 2009). The consecutive velocity increase was highest on the ice bridge (velocities nearly tripled at the narrowest part) and reached as far upstream as the Petrie Ice Rises (Fig. 2g). From the stress and strain fields in 2007, it seems unlikely that this acceleration was triggered by the collapse of the western bridge, because no significant restraint to the ice flow was transmitted via this branch. It seems more likely that the eastern branch weakened significantly by the loss of a small, but important area near the 1998 fracture pair. This area provided significant buttressing in 2007 (e.g., Fig. 3f). In 2008, the flow regime has significantly changed showing a steep increase in velocities along several line segments perpendicular to the ice-bridge orientation (passing by Vere Ice Rise). These discontinuities are ultimately transmitted to all derived quantities but are least expressed in the second principal strain component (Fig. 3l). In the homologue stress component, values turn positive in this area as compared to the 2007 state (Fig. 4g, h). Turning towards the remaining ice bridge, the in-flow strain-rates show different signs on each side of the narrowest bridge segment (Fig 3j). These observations explain why an initial crack formed there and the later failure position of the bridge (Humbert et al., 2010). The prevailing atmospheric circulation pushed the brittle ice mélange westward, which was the reason for why the bridge yielded in this direction (Humbert et al., 2010).

The narrow remainder of the ice bridge finally collapsed in April 2009 and an area of 330 km² broke-off (Humbert et al., 2010). This final event caused no further acceleration on the remnant WIS (Fig. 2h). This suggests that the lost ice-shelf portion did not transmit or provide much buttressing to the central ice-shelf unit. No field gives indication for further fracture opening.

In 2010, results from intensity-offset tracking were unavailable for some parts of the WIS and the coverage was incomplete (Fig. 2f). Yet, from the covered ice-shelf area, we are confident that ice flow did not change significantly between 2009 and 2010 (Fig. 2e, f). In addition, the ice-front position remained stable during this period (Fig. 2f).~~5 Conclusions~~

~~Our study revealed the potential of modern satellite missions to derive a comprehensive overview of dynamic changes on WIS before and during ice-shelf break-up. For this, multi-temporal velocity maps were derived for 1994/96 and 2006-2010. A considerable ice-flow speed up occurred after ice-front retreat in 2008. The estimation of principal strain-rate and stress components helped to identify ice-shelf areas prone to crevasse opening and fracture propagation during the individual stages of the ice bridge collapse between 2006 and 2009. These findings extend previous observations based on a qualitative analysis of satellite data. Directly inferable from surface velocities, the first principal strain rate as well as the strain rate in flow direction proofed valuable for interpreting the retreat stages. In terms of fracture initiation, the first principal surface stress could be exploited to infer where crevasses might open. However, this variable scales with the not well known ice viscosity. Independent of this scaling issue, positive values in the second principal surface stress highlight the regions susceptible to break-up. Other measures like second strain-rate regimes and the stress-flow angle proofed less appropriate to assess the subsequent retreat history and thus the ice-shelf stability.~~

The future stability of WIS is considered rather weak. Based on the analysis of several SAR images acquired in recent years (2011-2015) the formation of fractures at the south-western ice front was detected~~. In front of Lewis Snowfield, on the lee side of small ice rises,~~ (Fig. 1b). These fractures have developed since 2011 ~~(Fig. 1b)~~ and have grown perpendicular to the south-western ice front ~~since then.~~(Fig. 1b). In August 2014, one of these fractures grew further towards the centre of the ice shelf, forming a kink parallel to the south-western ice front. Another fracture was detected on a Sentinel~~-1a~~-1A imagery from April 2015, north of the ones described before (Fig. 1b). This fracture emerged perpendicular to the ice front towards the ice-shelf centre. Further growth of the fractures towards the ice-shelf centre and a connection of them, might lead to future loss of a large portion of the ice shelf and presumably a disconnection from Latady Island.

4.3 A-priori indications for retreat and fracturing

In this section, we want to investigate, which fields are most informative, when it comes to identifying weaknesses and predicting the next break-up stage. In 2006, no field shows any indication that another fracture pair would open. Yet, the existing fracture pair that formed in 1998 is discernible in most fields. This might simply imply that the integrity of the ice shelf was still unaffected and that a new zone of weakening was not yet established.

The opening of the fracture pair on the ice bridge in 2007 and the fracture formation perpendicular to the ice bridge in 2008, along which the later ice front formed, was best expressed in the ice velocities, both principal stress components, in the first principal strain-rates as well as in-flow strain-rates (Figs. 3&4). From the ice velocities a clear distinction can be made between a western and eastern flow branch on each side of the new fracture pair (Fig. 3e). Increased velocities at the western side indicate the subsequent failure of this part. For the derived quantities, this clear distinction is less evident as they are calculated from spatial derivatives. These fields rather give indications on the restraint or buttressing state. Magnitudes of stress and strain-rate components can be compared to threshold values for crevasse opening (Hambrey and Müller, 1978; Meier, 1958). Such a comparison is certainly intuitive for in-flow strain-rates. The more informative field, however, is the first principal strain as it holds the maximum extension. On the ice bridge in 2007 (Fig. 3g) and just upstream of its remainder in 2008 (Fig. 3k) first principal strain-rates reach values between ~$5 \cdot 10^{-5}$ and $1.3 \cdot 10^{-4}$ day^{-1}. The narrowest part of the ice bridge holds maximum first principal strain-rates of ~$1.2 \cdot 10^{-4}$ day^{-1} in 2008. These values compare to or even exceed threshold strain-rates inferred in areas where crevasses actually opened (Hambrey and Müller, 1978; Meier, 1958).

The first principal stress component also highlights regions, where fractures are likely to open or propagate (Krug et al., 2014; Vaughan, 1993). Threshold values for crevasse opening on various ice shelves fall into a range of 130 and 300 kPa as inferred by Vaughan (1993). For the break-up events in 2007 and 2008 (Figs. 4d, g), inferred stress values fall into this range. Values readily exceed ~200 kPa on the ice bridge in 2007. In 2008, similar values are found upstream of the ice bridge along the fractures that defined the successive ice-front position (Figs. 4d, g). Values were slightly lower at the narrowest part of the ice bridge, where the ice bridge collapse initiated (Fig. 4g). The interpretation of stress magnitudes is, however, limited as values directly scale with the rate factor choice. The second principal stress component shows some advantage in this respect (Fig. 4b, e, h, k). For all retreat stages, we confirm that this stress field shows a sign change to positive values in critical regions. Sign changes are scale-free and thus, unaffected by the rate factor choice.

For the interpretation of the second principal strain-rate component (Fig. 3, lowest panels), we want to follow Doake et al. (1998). They forwarded that when the ice front retreats beyond a certain 'compressive arch', the ice-shelf integrity is no longer granted and destabilization is expected. This strain-rate arch separates a seaward area of extension from an inland area of compression. The stress value associated to the 'compressive arch' isoline is not well quantified but "is probably close to the transition from extension to compression" (Doake et al., 1998) and thus, close to the zero isoline of the second principal strain-rate. On WIS, values are generally negative indicating unstable conditions, which is confirmed by general retreat. Yet, the threshold isoline is not clearly specified and might change in time and differ between ice shelves. Moreover, the second principal strain-rate field is found to be not very sensitive to ice-shelf fracturing and gradual ice-front recession, which appears unfavourable when assessing the dynamic state of an ice shelf.

Given the fact that the principal stresses and strain-rates are sufficient quantities for fracture hypothesis, a measure as the stress-flow angle does not lead to additional information for a fracture hypothesis. The distribution in Figure 4i also contradicts the observed consecutive collapse of the ice bridge. In addition, a more extensive retreat upstream of Vere Ice Rise is suggested by the stress-flow angle criterion in the state of 2008. To date, however, the north-eastern ice-front position as shown in 2009 remained unchanged. Further, no threshold value is given, which could serve to clearly delineate critical areas. Hence, the interpretation of stress-flow angles seems rather delicate und we suggest to use classical measures for fracture hypothesis like principal stress or strain criteria.

5 Conclusions

Our study revealed the potential of modern satellite missions to derive a comprehensive overview of dynamic changes on WIS before and during ice-shelf break-up. For this, time-series of ice velocity maps were derived for 1994/96 and 2006-2010. The most significant speed-up occurred in 2008 prior to the final collapse of an ice connection between Latady and Charcot Island. From velocities alone, we can only speculate that some flow restraint was removed during this event. Derived quantities such as in-flow and first principal strain-rates as well as principal stress components substantially help to identify areas of buttressing or areas prone to fracturing. First principal stress and strain-rates can be compared to previously forwarded threshold estimates for fracture opening on ice-shelves. The inferred stress field scales however with the poorly known rate factor, which complicates an interpretation.

Independent of this scaling issue, positive values in the second principal surface stress also highlight the regions susceptible to fracturing. Other measures proofed less appropriate to assess the retreat history on WIS. For the stress-flow angle, on the one hand, interpretation is less evident as no threshold is defined below which crevasse opening is notably facilitated. The second principal strain-rate, on the other hand, is mostly negative and thereby explains general retreat. Values are, however, rather insensitive for the detection of ice-shelf fracturing, even for the strong 2008 acceleration. Hence, this measure seems rather unfavourable when assessing the retreat stages of WIS.

This first assessment of which quantities are more or less meaningful with respect to predicting and describing dynamic changes on ice shelves could certainly be substantiated by assimilation of ice velocities into an ice flow model. Such an assimilation was unfortunately not possible as the ice-shelf thickness is not well known during the different retreat stages. The geometric evolution is important for a data assimilation on WIS as sub-shelf melt rates are very pronounced.

Author contributions

M.R. drafted the design of the study, collected the SAR data and calculated the velocity maps. J.F. calculated strain-rate and stress components as well as stress-flow angles. M.R. and J.F. analysed the results and wrote the manuscript jointly. The figures have been designed by M.R. The manuscript has been revised by M.B. and A.H. This work is embedded in a DFG project initiated by M.B. and A.H.

Acknowledgements

Satellite data was kindly provided by DLR AO mabra_XTI_GLAC0264 ~~and~~, ESA AO 4032 and AO 28292. The authors thank the Deutsche Forschungsgemeinschaft (DFG) for support in the framework of the priority program "Antarctic Research with comparative investigations in Arctic ice areas" under grant BR2105/8-1. M.B. received funding by the European Commission under the 7th Framework Program through the action – IMCONet (FP7 IRSES, action No.319718), J.F. was supported by DFG grant FU1032/1-1. This work was embedded as co-funding activity within the HGF Alliance "Remote Sensing & Earth System Dynamics".

References

Arigony-Neto, J., Skvarca, P., Marinsek, S., Braun, M., Humbert, A., Júnior, C. W. M. and Jaña, R.: Monitoring Glacier Changes on the Antarctic Peninsula, in Global Land Ice Measurements from Space, pp. 717–741, Springer., 2014.

Benn, D. I., Warren, C. R. and Mottram, R. H.: Calving processes and the dynamics of calving glaciers, Earth-Sci. Rev., 82(3), 143–179, 2007.

Berthier, E., Scambos, T. A. and Shuman, C. A.: Mass loss of Larsen B tributary glaciers (Antarctic Peninsula) unabated since 2002, Geophys. Res. Lett., 39(13), L13501, doi:10.1029/2012GL051755, 2012.

Braun, M. and Humbert, A.: Recent Retreat of Wilkins Ice Shelf Reveals New Insights in Ice Shelf Breakup Mechanisms, IEEE Geosci. Remote Sens. Lett., 6(2), 263–267, doi:10.1109/LGRS.2008.2011925, 2009.

Braun, M., Humbert, A. and Moll, A.: Changes of Wilkins Ice Shelf over the past 15 years and inferences on its stability, The Cryosphere, 3(1), 41–56, doi:10.5194/tc-3-41-2009, 2009.

Bromirski, P. D., Sergienko, O. V. and MacAyeal, D. R.: Transoceanic infragravity waves impacting Antarctic ice shelves: IG-WAVES IMPACTING ANTARCTIC ICE SHELVES, Geophys. Res. Lett., 37(2), doi:10.1029/2009GL041488, 2010.

Burgess, E. W., Forster, R. R., Larsen, C. F. and Braun, M.: Surge dynamics on Bering Glacier, Alaska, in 2008–2011, The Cryosphere, 6(6), 1251–1262, doi:10.5194/tc-6-1251-2012, 2012.

Cook, A. J.: Retreating Glacier Fronts on the Antarctic Peninsula over the Past Half-Century, Science, 308(5721), 541–544, doi:10.1126/science.1104235, 2005.

Cuffey, K. M. and Paterson, W. S. B.: The physics of glaciers, Academic Press., 2010.

De Angelis, H. and Skvarca, P.: Glacier surge after ice shelf collapse, Science, 299(5612), 1560–1562, 2003.

Doake, C. S. M. and Vaughan, D. G.: Rapid disintegration of the Wordie Ice Shelf in response to atmospheric warming, Nature, 350(6316), 328–330, doi:10.1038/350328a0, 1991.

Doake, C. S. M., Corr, H. F. J., Rott, H., Skvarca, P. and Young, N. W.: Breakup and conditions for stability of the northern Larsen Ice Shelf, Antarctica, Nature, 391(6669), 778–780, 1998.

Drews, R., Rack, W., Wesche, C. and Helm, V.: A spatially adjusted elevation model in Dronning Maud Land, Antarctica, based on differential SAR interferometry, IEEE Trans. Geosci. Remote Sens., 47(8), 2501–2509, 2009.

Dupont, T. K. and Alley, R. B. Assessment of the importance of ice-shelf buttressing to ice-sheet flow. Geophysical Research Letters. 32, L04503, 2005.

Fricker, H. A. and Padman, L.: Thirty years of elevation change on Antarctic Peninsula ice shelves from multimission satellite radar altimetry, J. Geophys. Res., 117(C2), doi:10.1029/2011JC007126, 2012.

Fürst, J. J., Durand, G., Gillet-Chaulet, F., Tavard, L., Rankl, M., Braun, M. and Gagliardini, O.: The safety band of Antarctic ice shelves, Nat. Clim Change, 6(5), 479–482, 2016.

Gray, A. L., Mattar, K. E. and Sofko, G.: Influence of ionospheric electron density fluctuations on satellite radar interferometry, Geophys. Res. Lett., 27(10), 1451–1454, doi:10.1029/2000GL000016, 2000.

Gross, D., Hauger, Werner and Wriggers, Peter: Technische Mechanik: Band 4: Hydromechanik, 8th ed., Springer, Berlin, 2009.

Hambrey, M. J. and Müller, F.: Structures and ice deformation in the white glacier, Axel Heiberg Island, Northwest Territories, Canada, J. Glaciol., 20(82), 41–66, 1978.

Holland, P. R., Jenkins, A. and Holland, D. M.: Ice and ocean processes in the Bellingshausen Sea, Antarctica, J. Geophys. Res., 115(C5), doi:10.1029/2008JC005219, 2010.

Humbert, A. and Braun, M.: The Wilkins Ice Shelf, Antarctica: break-up along failure zones, J. Glaciol., 54(188), 943–944, doi:10.3189/002214308787780012, 2008.

Humbert, A., Gross, D., Müller, R., Braun, M., Van De Wal, R. S. W., Van Den Broeke, M. R., Vaughan, D. G. and Van De Berg, W. J.: Deformation and failure of the ice bridge on the Wilkins Ice Shelf, Antarctica, Ann. Glaciol., 51(55), 49–55, 2010.

~~Jansen, D., Luckman, A. J., Cook, A., Bevan, S., Kulessa, B., Hubbard, B. and Holland, P. R.: Brief Communication: Newly developing rift in Larsen C Ice Shelf presents significant risk to stability, The Cryosphere, 9(3), 1223–1227, doi:10.5194/tc-9-1223-2015, 2015.~~

Jezek, K., John Curlander, Frank Carsey, Carl Wales, and R.Barry: RAMP AMM-1 SAR Image Mosaic of Antarctica, Version 2, doi:10.5067/8AF4ZRPULS4H, 2013.

Khazendar, A., Borstad, C. P., Scheuchl, B., Rignot, E. and Seroussi, H.: The evolving instability of the remnant Larsen B Ice Shelf and its tributary glaciers, Earth Planet. Sci. Lett., 419, 199–210, doi:10.1016/j.epsl.2015.03.014, 2015.

Krug, J., Weiss, J., Gagliardini, O. and Durand, G.: Combining damage and fracture mechanics to model calving, The Cryosphere, 8(6), 2101–2117, 2014.

Kulessa, B., Jansen, D., Luckman, A. J., King, E. C. and Sammonds, P. R.: Marine ice regulates the future stability of a large Antarctic ice shelf, Nat. Commun., 5, 2014.

MacAyeal, D. R., Scambos, T. A., Hulbe, C. L. and Fahnestock, M. A.: Catastrophic ice-shelf break-up by an ice-shelf-fragment-capsize mechanism, J. Glaciol., 49(164), 22–36, 2003.

Martinson, D. G., Stammerjohn, S. E., Iannuzzi, R. A., Smith, R. C. and Vernet, M.: Western Antarctic Peninsula physical oceanography and spatio–temporal variability, Deep Sea Res. Part II Top. Stud. Oceanogr., 55(18), 1964–1987, 2008.

Mcnabb, R. W., Hock, R., O'Neel, S., Rasmussen, L. A., Ahn, Y., Braun, M., Conway, H., Herreid, S., Joughin, I., Pfeffer, W. T., Smith, B. E. and Truffer, M.: Using surface velocities to calculate ice thickness and bed topography: a case study at Columbia Glacier, Alaska, USA, J. Glaciol., 58(212), 1151–1164, doi:10.3189/2012JoG11J249, 2012.

Meier, M. F.: The mechanics of crevasse formation, Gen. Assem. Tor. 1957-Snow Ice, 46, 500–508, 1958.

Meredith, M. P. and King, J. C.: Rapid climate change in the ocean west of the Antarctic Peninsula during the second half of the 20th century, Geophys. Res. Lett., 32(19), 2005.

~~Meyer, F., Bamler,~~Nagler, T., Rott, H., Hetzenecker, M., Wuite, J.~~ R., Jakowski, N.~~ and ~~Fritz, T~~Potin, P.: The ~~Potential of Low-Frequency SAR Systems~~Sentinel-1 Mission: New Opportunities for ~~Mapping Ionospheric TEC Distributions, IEEE~~ Ice Sheet Observations, ~~Geosci.~~ Remote Sens~~. Lett., 3(4), 560–564~~., 7(7), 9371–9389, doi:10.~~1109/LGRS.2006.882148, 2006~~3390/rs70709371, 2015.

O'Donnell, R., Lewis, N., McIntyre, S. and Condon, J.: Improved methods for PCA-based reconstructions: Case study using the Steig et al.(2009) Antarctic temperature reconstruction, J. Clim., 24(8), 2099–2115, 2011.

Padman, L., Costa, D. P., Dinniman, M. S., Fricker, H. A., Goebel, M. E., Huckstadt, L. A., Humbert, A., Joughin, I., Lenaerts, J. T. M., Ligtenberg, S. R. M., Scambos, T. and van den Broeke, M. R.: Oceanic controls on the mass balance of Wilkins Ice Shelf, Antarctica, J. Geophys. Res., 117(C1), doi:10.1029/2011JC007301, 2012.

Paolo, F. S., Fricker, H. A. and Padman, L.: Volume loss from Antarctic ice shelves is accelerating, Science, 348(6232), 327–331, doi:10.1126/science.aaa0940, 2015.

~~Pattyn, F.: A new three-dimensional higher-order thermomechanical ice sheet model: Basic sensitivity, ice stream development, and ice flow across subglacial lakes, J. Geophys. Res. Solid Earth, 108(B8), 2003.~~

Pralong, A., Hutter, K. and Funk, M.: Anisotropic damage mechanics for viscoelastic ice, Contin. Mech. Thermodyn., 17(5), 387–408, doi:10.1007/s00161-005-0002-5, 2006.

Quincey, D. J., Copland, L., Mayer, C., Bishop, M., Luckman, A. and Belo, M.: Ice velocity and climate variations for Baltoro Glacier, Pakistan, J. Glaciol., 55(194), 1061–1071, 2009.

Quincey, D. J., Braun, M., Glasser, N. F., Bishop, M. P., Hewitt, K. and Luckman, A.: Karakoram glacier surge dynamics, Geophys. Res. Lett., 38(18), L18504, doi:10.1029/2011GL049004, 2011.

Rignot, E.: Accelerated ice discharge from the Antarctic Peninsula following the collapse of Larsen B ice shelf, Geophys. Res. Lett., 31(18), doi:10.1029/2004GL020697, 2004.

Rignot, E., Jacobs, S., Mouginot, J. and Scheuchl, B.: Ice-Shelf Melting Around Antarctica, Science, 341(6143), 266–270, doi:10.1126/science.1235798, 2013.

Robertson, R., Visbeck, M., Gordon, A. L. and Fahrbach, E.: Long-term temperature trends in the deep waters of the Weddell Sea, Deep Sea Res. Part II Top. Stud. Oceanogr., 49(21), 4791–4806, 2002.

Rott, H., Rack, W., Skvarca, P. and De Angelis, H.: Northern Larsen ice shelf, Antarctica: further retreat after collapse, Ann. Glaciol., 34(1), 277–282, 2002.

Scambos, T., Hulbe, C. and Fahnestock, M.: Climate-Induced Ice Shelf Disintegration in the Antarctic Peninsula, in Antarctic Peninsula Climate Variability: Historical and Paleoenvironmental Perspectives, edited by E. Domack, A. Levente, A. Burnet, R. Bindschadler, P. Convey, and tthew Kirby, pp. 79–92, American Geophysical Union. [online] Available from: http://onlinelibrary.wiley.com/doi/10.1029/AR079p0079/summary (Accessed 26 September 2014), 2003.

Scambos, T., Fricker, H. A., Liu, C.-C., Bohlander, J., Fastook, J., Sargent, A., Massom, R. and Wu, A.-M.: Ice shelf disintegration by plate bending and hydro-fracture: Satellite observations and model results of the 2008 Wilkins ice shelf break-ups, Earth Planet. Sci. Lett., 280(1–4), 51–60, doi:10.1016/j.epsl.2008.12.027, 2009.

Scambos, T. A.: Glacier acceleration and thinning after ice shelf collapse in the Larsen B embayment, Antarctica, Geophys. Res. Lett., 31(18), doi:10.1029/2004GL020670, 2004.

Scambos, T. A., Hulbe, C., Fahnestock, M. and Bohlander, J.: The link between climate warming and break-up of ice shelves in the Antarctic Peninsula, J. Glaciol., 46(154), 516–530, 2000.

Scambos, T. A., Berthier, E., Haran, T., Shuman, C. A., Cook, A. J., Ligtenberg, S. R. M. and Bohlander, J.: Detailed ice loss pattern in the northern Antarctic Peninsula: widespread decline driven by ice front retreats, The Cryosphere, 8(6), 2135–2145, doi:10.5194/tc-8-2135-2014, 2014.

Seehaus, T., Marinsek, S., Helm, V., Skvarca, P. and Braun, M.: Changes in ice dynamics, elevation and mass discharge of Dinsmoor–Bombardier–Edgeworth glacier system, Antarctic Peninsula, Earth Planet. Sci. Lett., 427, 125–135, doi:10.1016/j.epsl.2015.06.047, 2015.

Shuman, C. A., Berthier, E. and Scambos, T. A.: 2001–2009 elevation and mass losses in the Larsen A and B embayments, Antarctic Peninsula, J. Glaciol., 57(204), 737–754, doi:10.3189/002214311797409811, 2011.

Stammerjohn, S. E., Martinson, D. G., Smith, R. C., Yuan, X. and Rind, D.: Trends in Antarctic annual sea ice retreat and advance and their relation to El Niño–Southern Oscillation and Southern Annular Mode variability, J. Geophys. Res. Oceans 1978–2012, 113(C3), 2008.

Steig, E. J., Schneider, D. P., Rutherford, S. D., Mann, M. E., Comiso, J. C. and Shindell, D. T.: Warming of the Antarctic ice-sheet surface since the 1957 International Geophysical Year, Nature, 457(7228), 459–462, 2009.

Strozzi, T., Luckman, A., Murray, T., Wegmuller, U. and Werner, C. .: Glacier motion estimation using SAR offset-tracking procedures, Geosci. Remote Sens. IEEE Trans. On, 40(11), 2384–2391, 2002.

Van der Veen, C. J.: Fundamentals of glacier dynamics, CRC Press, Rotterdam, The Netherlands., 2013.

Vaughan, D. G.: Relating the occurrence of crevasses to surface strain rates, J. Glaciol., 39, 255–266, 1993.

Vaughan, D. G. and Doake, C. S. M.: Recent atmospheric warming and retreat of ice shelves on the Antarctic Peninsula, 1996.

Vaughan, D. G., Mantripp, D. R., Sievers, J. and Doake, C. S. M.: A synthesis of remote sensing data on Wilkins Ice Shelf, Antarctica, Ann. Glaciol., 17, 211–218, 1993.

Vaughan, D. G., Marshall, G. J., Connolley, W. M., Parkinson, C., Mulvaney, R., Hodgson, D. A., King, J. C., Pudsey, C. J. and Turner, J.: Recent rapid regional climate warming on the Antarctic Peninsula, Clim. Change, 60(3), 243–274, 2003.

Wouters, B., Martin-Español, A., Helm, V., Flament, T., van Wessem, J. M., Ligtenberg, S. R. M., van den Broeke, M. R. and Bamber, J. L.: Dynamic thinning of glaciers on the Southern Antarctic Peninsula, Science, 348(6237), 899–903, doi:10.1126/science.aaa5727, 2015.

Werner, C., Wegmüller, U., Strozzi, T. and Wiesmann, A.: Gamma SAR and interferometric processing software, in Proc. ERS-ENVISAT Symposium, Gothenburg, Sweden, 16–20 October 2000, 2000.

Williams, S., Bock, Y. and Fang, P.: Integrated satellite interferometry: Tropospheric noise, GPS estimates and implications for interferometric synthetic aperture radar products, J. Geophys. Res., 103(B11), 27051–27067, 1998.

Zwally, H. J., Giovinetto, M. B., Jun, L., Cornejo, H. G., Beckley, M. A., Brenner, A. C., Saba, J. L. and Yi, D.: Mass changes of the Greenland and Antarctic ice sheets and shelves and contributions to sea-level rise: 1992–2002, J. Glaciol., 51(175), 509–527, doi:10.3189/172756505781829007, 2005

Table 1: Parameter settings used for SAR intensity-offset tracking.

Sensor	Sensor wavelength	Tracking window size (range * azimuth)	Step (range/azimuth)
ALOS PALSAR	23.5 cm L-band	128*384	12/36
ERS-1/2 SAR	5.6 cm C-band	256*1280	15/75

Table 2: Error estimation of derived velocity fields.

Date	Sensor	σ_v^C	σ_v^T	σ_v
yyyy-mm-dd--yyyy-mm-dd		[m/d]	[m/d]	[m/d]
1994-03-02--1994-03-17	ERS SAR	0,0645311	0,2	0,2645311
2006-05-18--2006-07-03	ALOS PALSAR	0,0707297	0,03	0,1007297
2006-06-09--2006-07-25	ALOS PALSAR	0,249185	0,03	0,279185
2006-06-14--2006-07-30	ALOS PALSAR	0,267962	0,03	0,297962
2007-09-26--2007-11-11	ALOS PALSAR	0,25396	0,03	0,28396
2007-09-28--2007-11-13	ALOS PALSAR	0,1755955	0,03	0,2055955
2007-10-20--2007-12-05	ALOS PALSAR	0,0428592	0,03	0,0728592
2008-09-18--2008-11-03	ALOS PALSAR	0,186815	0,03	0,216815
2008-09-28--2008-11-13	ALOS PALSAR	0,113365	0,03	0,143365
2008-10-22--2008-12-07	ALOS PALSAR	0,037087	0,03	0,067087
2009-09-09--2009-10-25	ALOS PALSAR	0,06461115	0,03	0,09461115
2009-09-21--2009-11-06	ALOS PALSAR	0,0428839	0,03	0,0728839
2009-10-01--2009-11-16	ALOS PALSAR	0,1476365	0,03	0,1776365
2010-08-09--2010-09-24	ALOS PALSAR	0,04809755	0,03	0,07809755
2010-09-29--2010-11-14	ALOS PALSAR	0,0657041	0,03	0,0957041
2010-10-09--2010-11-24	ALOS PALSAR	0,08	0,03	0,11

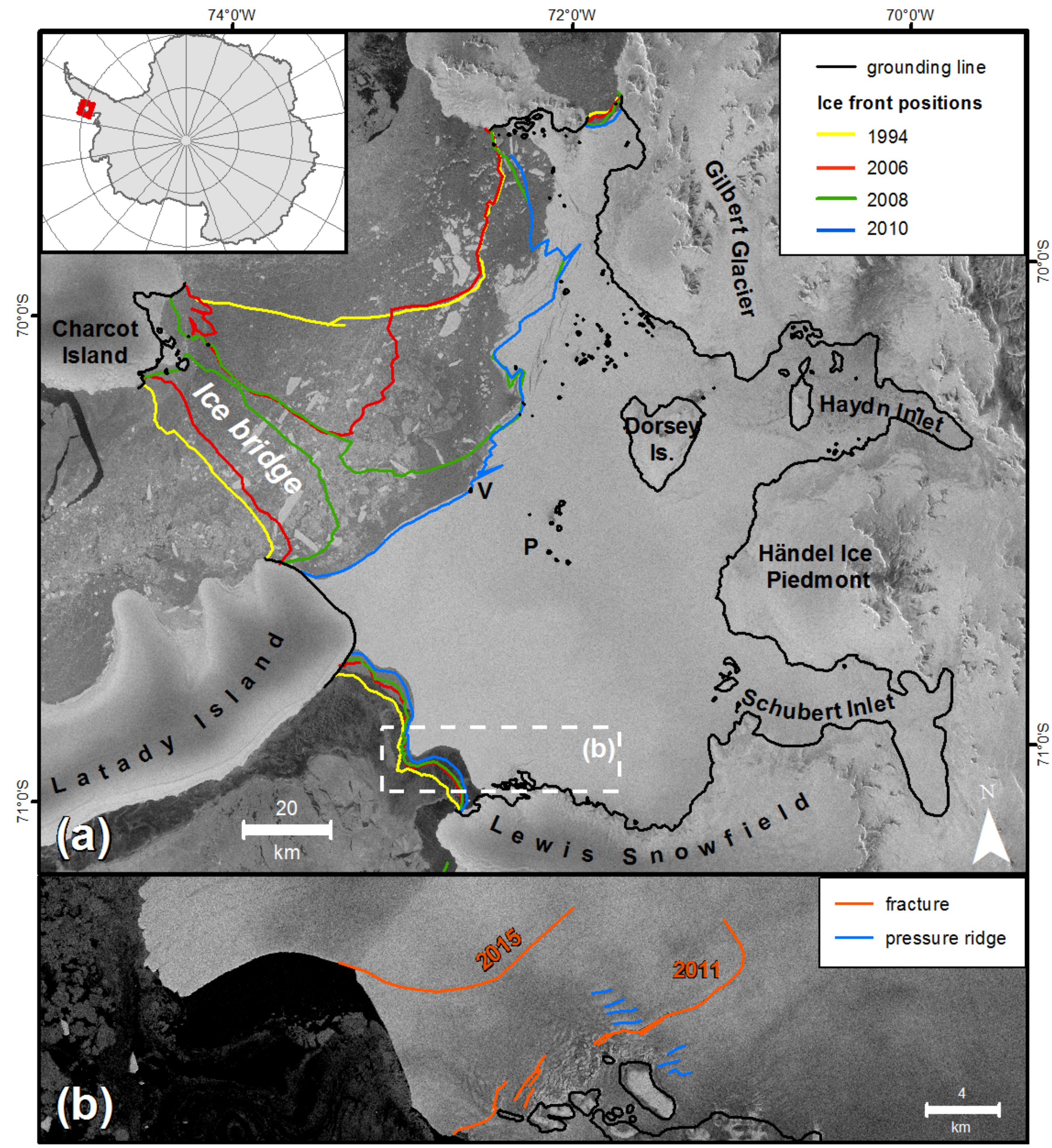

Figure 1: (a) Overview map of Wilkins Ice Shelf. The ice-front positions of the years 1994 and 2008 as well as the situation in 2015 are shown. The remnant ice connection (ice bridge) between Charcot and Latady Island in its shape from April 2008 is indicated. The location of the grounding line was derived from ERS-1/-2 differential interferometry (supplement material S3). (b) Fracture formation at the south-western ice front as detected between 2011 and 2015 from Envisat ASAR, Sentinel 1a and TanDEM-X imagery. P = Petrie Ice Rises, V = Vere Ice Rise. Background: Sentinel 1a 21-05-2015 © ESA.

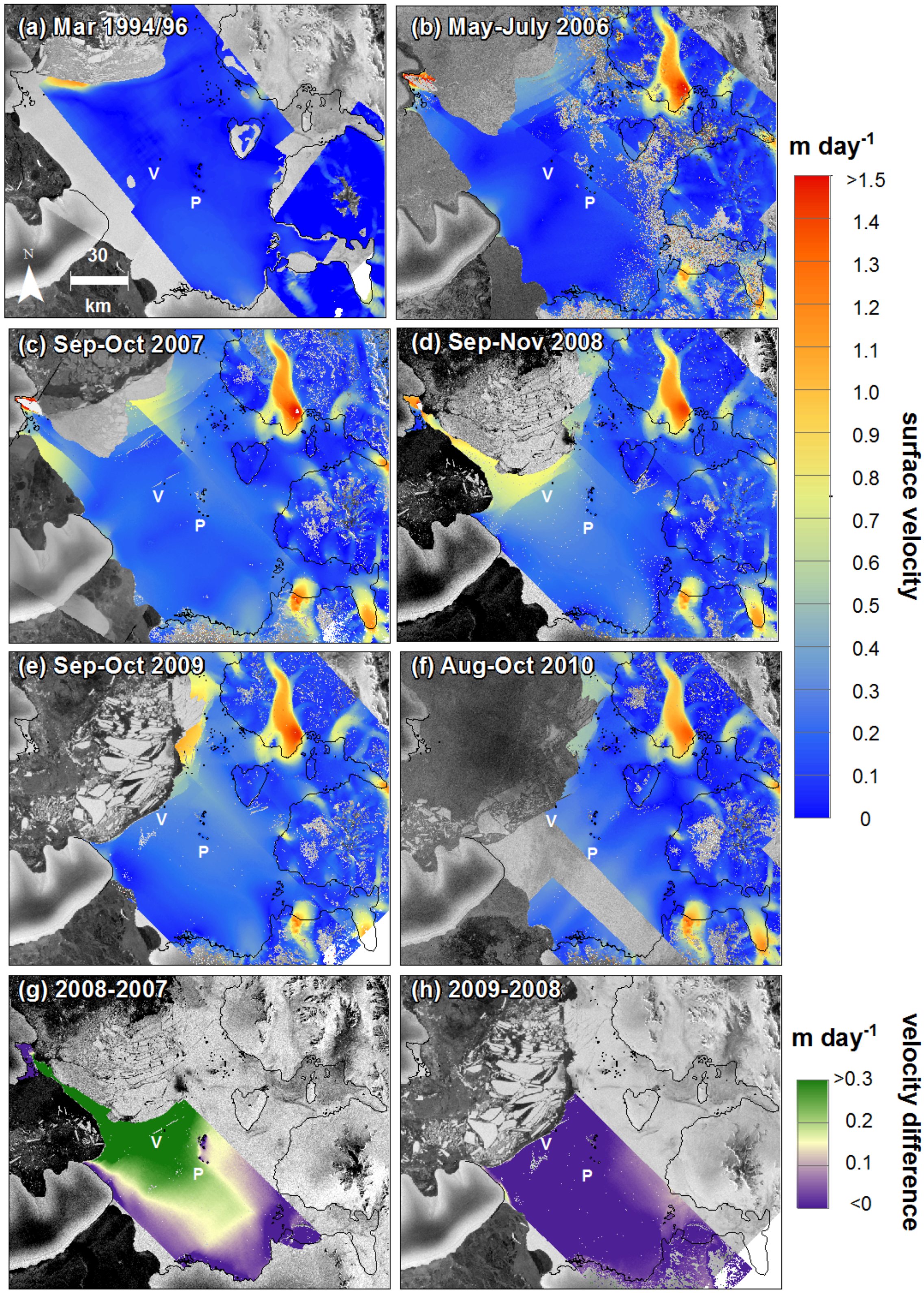

Figure 2: Surface velocities of WIS in 1994/96 and between 2006 and 2010 derived from ERS-1/2 (Braun et al., 2009) and ALOS PALSAR intensity-offset tracking. The position of the grounding line in 1995/96 is marked as black line. Panels g) and h) show differences in surface flow between 2008 and 2007, and 2009 and 2008, respectively, for the western part of the ice shelf. P = Petrie Ice Rises, V = Vere Ice Rise. Background imagery: (a) ~~MOA 2003/2004 © NSIDC,~~RAMP Mosaic Sep./Oct. 1997 (Jezek, 2013), ERS-1/2 SAR 19-08-1993; (b) Envisat ASAR 25-03-2006; (c) Envisat ASAR 05-08-2007 and 09-09-2007; (d) Envisat ASAR 25-08-2008; (e) Envisat ASAR 22-07-2009; (f) Envisat ASAR 09-12-2010; (g) Envisat ASAR 25-08-2008; (h) Envisat ASAR 22-07-2009, © ESA.

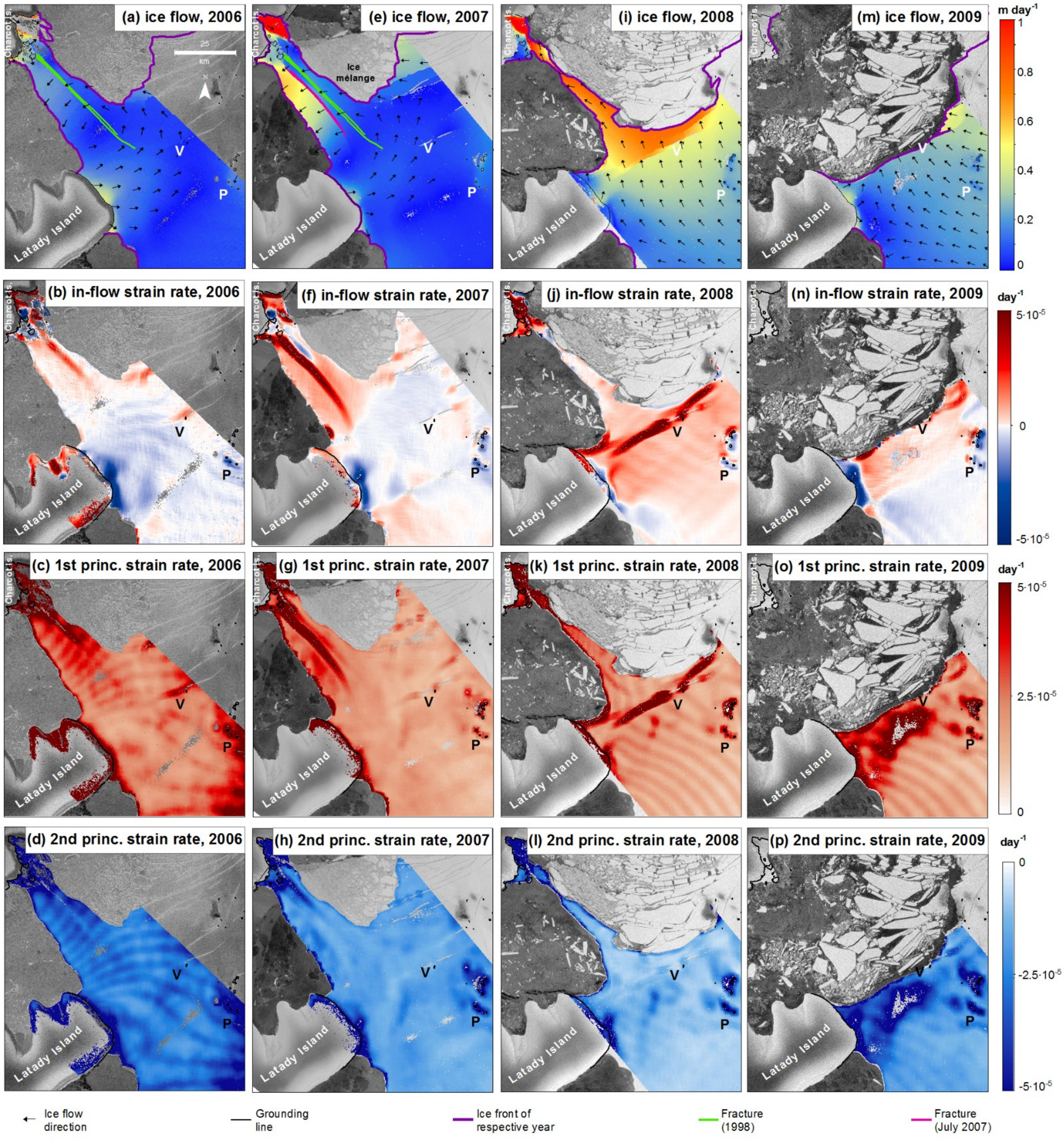

Figure 3: Surface velocities (first row), strain-rates in flow direction (second row), first and second principal strain-rates for the years 2006-2009 (bottom rows). For depiction, the strain-rate components were filtered using a moving average with a rectangular kernel of 1000m x 1000m. Arrows show the ice-flow direction above a threshold of 0.05 m day^{-1}. For each date the respective ice-front positions are shown. A double fracture system formed in 1998 is shown as green lines in (a) and (e). ~~A newly~~Another fracture pair developed ~~double fracture formed~~ in July 2007 is marked as purple line in (e). P = Petrie Ice Rises, V = Vere Ice Rise. Background imagery: (a)-(d) Envisat ASAR 25-03-2006; (e)-(h) Envisat ASAR 09-09-2007; (i)-(l) Envisat ASAR 02-08-2008/06-08-2008; (m)-(p) Envisat ASAR 22-07-2009; © ESA.

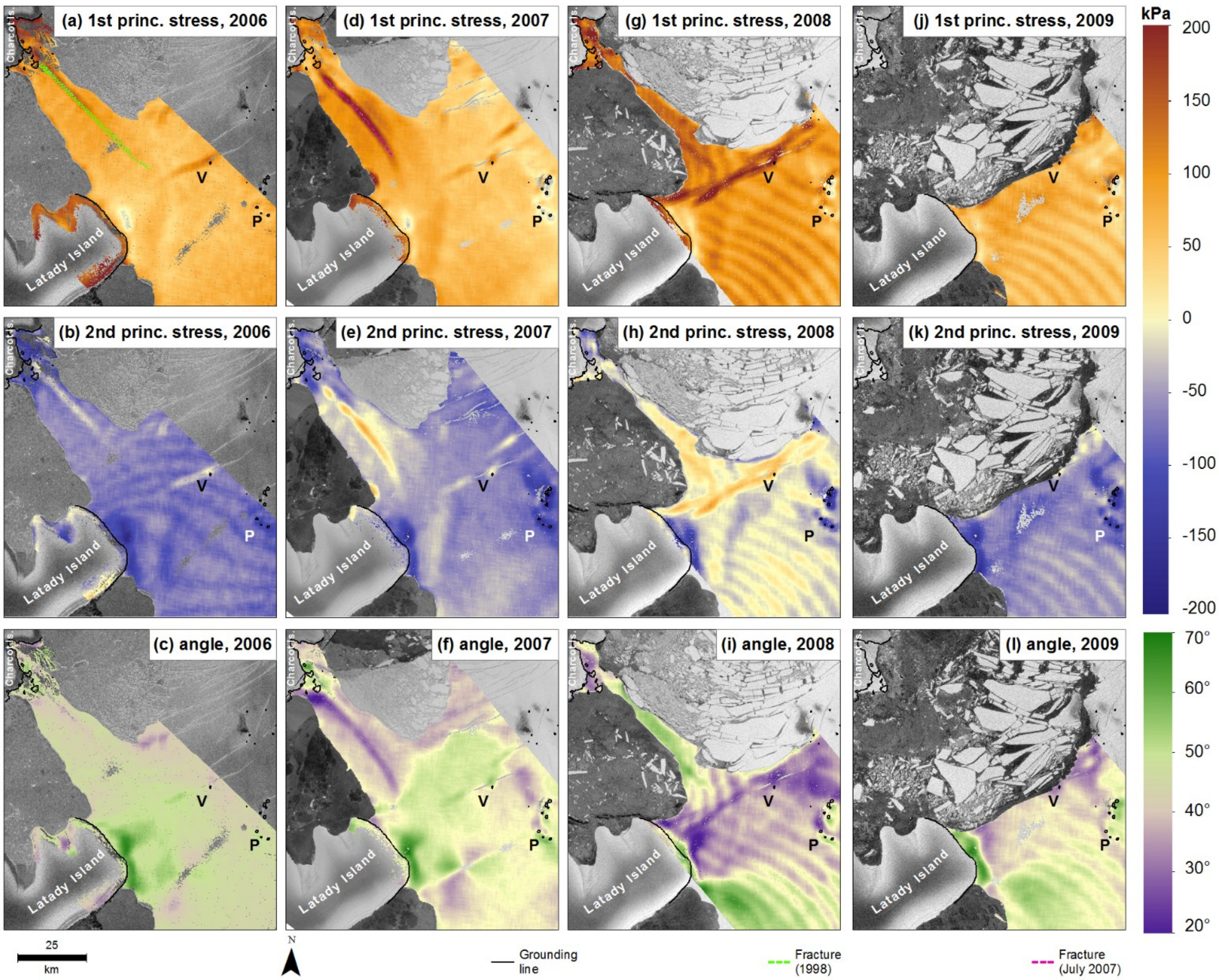

Figure 4: First and second principal stress fields as well as stress-flow angles on WIS for the years 2006-2009. P = Petrie Ice Rises, V = Vere Ice Rise. Background imagery: (a)-(c) Envisat ASAR 25-03-2006; (d)-(f) Envisat ASAR 09-09-2007; (g)-(i) Envisat ASAR 02-08-2008/06-08-2008; (j)-(l) Envisat ASAR 22-07-2009; © ESA.